

<https://doi.org/10.1038/s44296-024-00021-z>

Multiscale perspectives for advancing sustainability in fiber reinforced ultra-high performance concrete

Check for updates

Xing Quan Wang, Cheuk Lun Chow & Denvi Lau

Ultra-high performance concrete (UHPC) integrates cutting-edge nano-additives, fibers and cementitious materials, which is a representative heterogeneous material and exhibits distinctive multi-scale structural characteristics. With remarkable durability and mechanical properties, lower embodied energy and diminished carbon emissions compared to conventional concrete, the application of UHPC aligns with the principles of sustainable development. To accelerate these advances, researchers of construction materials have incorporated a multiscale perspective into UHPC studies. From the perspective of sustainability, we evaluate the latest advances in the design, application and innovation of UHPC under multiscale perspective. Based on the fundamentals of fiber-reinforced UHPC, we discuss why and how could multiscale mechanics research, including analytical and modeling methods helps the advances of its sustainability, emphasizing the ecological considerations of UHPC in the practical applications. Then we summarize the challenges and perspectives in the design, production and construction of UHPC materials and structures. Based on advances in multiscale mechanics, a bright future can be envisioned where sustainable UHPC is applied globally, led by additive manufacturing and artificial intelligence.

Concrete, a widely employed construction material, exhibits inherent limitations such as low tensile strength, brittleness, insufficient strain capacity and strain capacity¹⁻³. To address these concerns, the reinforcement of concrete with diverse fibers, including metallic, synthetic, carbon, and mineral fibers, has been pursued to augment its toughness. In response to the growing demand for high-strength and durable concrete, a type of advanced fiber-reinforced concrete was developed in the mid-1990s that has been titled ultra-high performance concrete (UHPC)⁴. UHPC features the high-density microstructure and mechanical properties which possess compressive strength above 150 MPa and flexural strength over 50 MPa⁵⁻⁷. UHPC also demonstrates exceptional hardened and durability properties, including remarkable self-compactness properties, enhanced structural ductility, pseudo-strain hardening behaviors, bond strength, as well as superior resistance to aggressive environmental conditions than normal concrete⁸⁻¹¹. UHPC consists of a large volume of cement, silica fume, fibers, superplasticizers and other supplementary cementitious materials (SCMs), which formulation aims to improve toughness, durability, homogeneity, and reduce porosity¹²⁻¹⁴. Different from normal FRC, UHPC is designed by the dense packing theory of solid materials, involves a high cement content

with the low water-to-binder (w/b) ratio, and micro-scale fibers¹⁴. Given UHPC's efficient resource utilization and reduced maintenance requirements, it emerges as a plausible strategy for mitigating the adverse effects associated with conventional construction methods. Although the energy and economic costs of UHPC are high, the high initial investment would be offset by the reduction of maintenance costs as UHPC has better properties than conventional concrete and a longer service life^{15,16}. Given UHPC's exceptional strength-to-weight ratio, it emerges as an economically viable choice for the design and construction of new concrete structures¹⁷. This characteristic enables the reduction in the size of structural members and the increased spacing between them, as well as the potential for the restoration of pre-existing buildings¹⁸. Hence, the overall cement consumption during construction is reduced. Reducing cement usage in UHPC not only significantly contributes to cost and CO₂ emission reductions but also promotes sustainability in the construction sector by minimizing environmental impacts and providing eco-efficient construction materials¹⁹.

Enhancing the performance and managing costs of UHPC has long been a focal point of existing studies. The pursuit of performance improvement involves the removal of coarse aggregates, incorporating

Department of Architecture and Civil Engineering, City University of Hong Kong, Hong Kong, China.

 e-mail: denvi.lau@cityu.edu.hk

advanced additives, using high-range water-reducing admixtures, and optimizing mix proportions and the granular matrix. These efforts are aimed at improving the mechanical properties, durability, and sustainability of UHPC, thereby expanding its potential applications in various structural and infrastructure projects. Moreover, the broader utilization of UHPC in the construction industry has been limited by its relatively high initial cost. Ongoing investigations are actively addressing knowledge gaps and paving the way for the development of innovative UHPC formulations that offer reduced initial costs. Concurrently, the elevated cost of UHPC raw materials and the intricate curing process involving steam or extreme heating necessitate substantial energy consumption. This notable energy demand significantly contributes to the higher price associated with industrial manufacturing of UHPC compared to water curing. Therefore, extensive efforts are required to address these challenges, starting from the optimization of UHPC's composition and concluding with the development of energy-efficient and cost-effective production processes for UHPC to improve its sustainability and durability.

The development of multiscale mechanical theories and modeling techniques specific to UHPC is crucial and foundational for advancing UHPC towards greater sophistication, sustainability, and environmental friendliness^{20,21}. The performance of UHPC is closely related to the content, properties, distribution patterns, and interface characteristics of its various components²². With the advancement of manufacturing techniques and the development of nanotechnology^{23,24}, the introduction of micro- and nano-scale components has further enhanced the performance of UHPC, while simultaneously enriching its composition and increasing the complexity of its hierarchical structure as shown in Fig. 1. For such complex cementitious composite materials, the conventional continuum mechanics theory struggles to account for their intricate features, while the suitable range of scales for applying the micromechanics approach remains to be explored^{25,26}. Therefore, the efficient and accurate prediction of the macroscopic performance of UHPC based on its micro- and nano-scale information, as well as the design and optimization of its micro- and nano-structure according to the required macroscopic performance for practical applications²⁷, has become a pivotal topic in UHPC-related research. Hence, it is imperative to have multiscale perspective in the investigation of the sustainability and durability of UHPC, aiming to establish quantitative relationships between its macroscopic performance and the nano-, micro-, and other hierarchical structures. Multiscale mechanics methods rely on the microscopic structural information of materials. Currently, the available methods for mechanical analysis at the microscopic scale include first-principles calculations and Molecular Dynamics (MD). Among them, MD is a nanoscale simulation method based on interatomic interactions^{28,29}. Extensive research has demonstrated that MD simulations can effectively

elucidate deformation and failure mechanisms of materials^{30–34}, thereby establishing a crucial physical foundation for cross-scale mechanical analysis³⁵. For bridging atomistic scale to continuum scale, the quasi-continuum method³⁶, the handshake method³⁷, and the coarse-grained (CG) method³⁸ are widely employed.

We systematically review the recent progress in advancing sustainability in UHPC under multiscale perspectives, with an emphasis on how multiscale theories and modeling techniques address the challenges in the ecological considerations of UHPC. We first summarize the fundamentals of UHPC and discuss the influence of fiber types (i.e. steel, carbon, mineral, cellulose, synthetic) and geometric characteristics (i.e. length, shapes, distributions, and orientations of fibers) on the properties of UHPC³⁹. Based on the peculiarities of the sustainability of UHPC, special attention has been given to the applications of multiscale theories and modeling techniques in emerging low-carbon strategies and sustainable design. Finally, we identify areas in which multiscale techniques have the potential for accelerating sustainable research and consider the ecological developments of UHPC in practical applications.

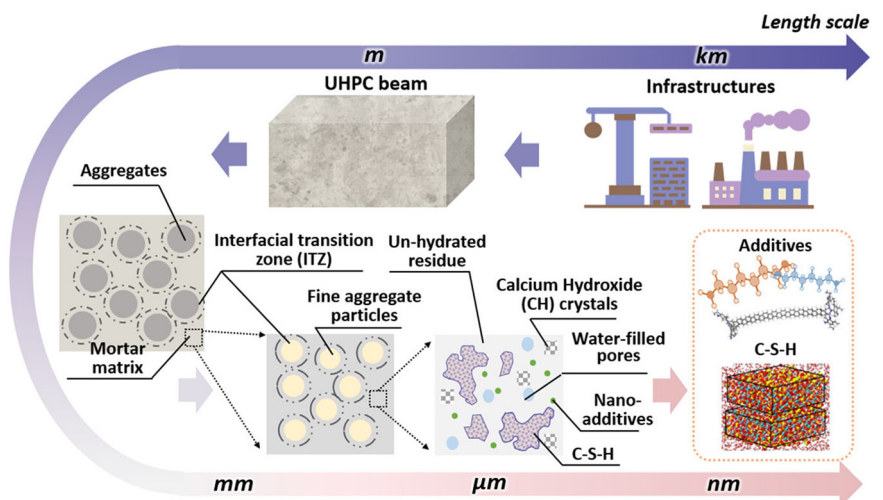
Fundamentals of fiber-reinforced UHPC

Basic principles for improving performance

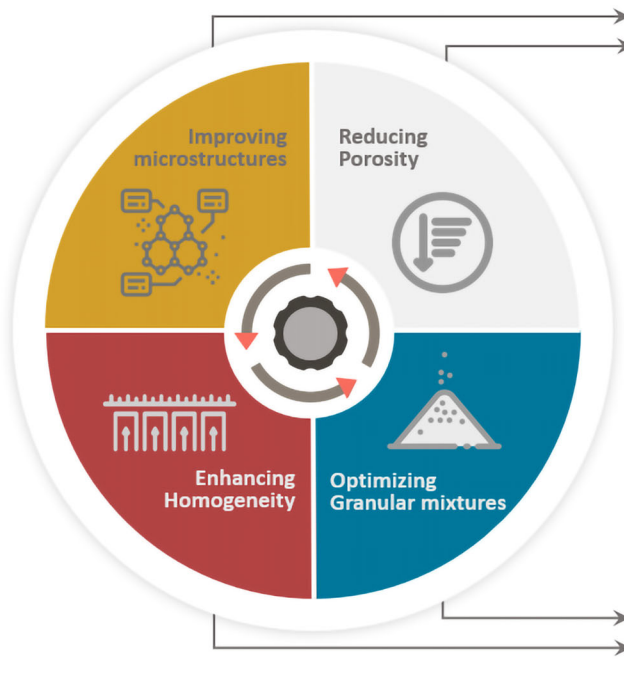
Significant advancements and refinements have been made in the fundamental principles of UHPC architecture over the past few decades, laying a solid foundation for its further development^{4,40}. With the continuous advancement of relevant research, UHPC is widely applied due to its exceptional performance and the versatility of additives that can be utilized to enhance UHPC properties and overcome its limitations. The fundamental philosophy of enhancing its performance encompasses reducing the porosity, improving the microstructures, enhancing homogeneity and optimizing granular mixtures, as shown in Fig. 2^{41,42}. These factors are highly dependent on the raw materials and mixture design of UHPC.

To reduce the porosity and improve the microstructure of UHPC, optimal mixture proportion designs should be developed^{43,44}. The commonly used strategy involves relies on application of fibers and mineral additives, which can create the matrix with low porosity, higher strength, better failure behavior, and improve compressive strength of UHPC to 150–200 MPa^{29,45–48}. The used fibers for the development of UHPC are summarized in Table 1, which evaluates the tensile strength and Young's modulus of different fibers employed in concrete, providing a comparative analysis^{49–51}. Although dozens of different fibers are used in UHPC, they can generally be divided into three types based on texture: metallic fibers (i.e. steel fibers), synthetic fibers, and mineral fibers⁵². Among those, steel, polyethylene (PE), polyvinyl alcohol (PVA), polypropylene (PP), carbon, and basalt are the prevailing fiber types employed in UHPC. In metallic

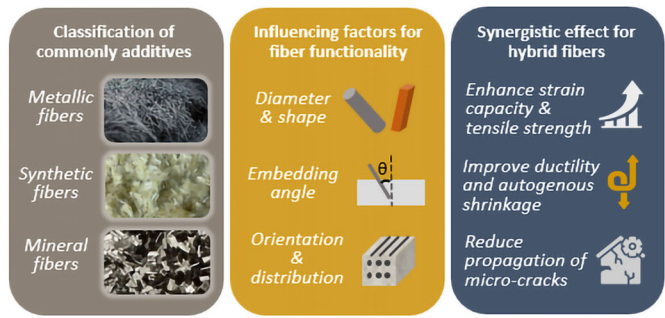
Fig. 1 | Schematic diagram for the multiscale hierarchical structure of UHPC. UHPC is a representative heterogeneous material, exhibits distinctive structural characteristics under different length scale.



Improving Performance of Fiber-reinforced UHPC



(A) FIBER/ADDITIVES-RELATED APPROACHES



(B) MATRIX-RELATED APPROACHES

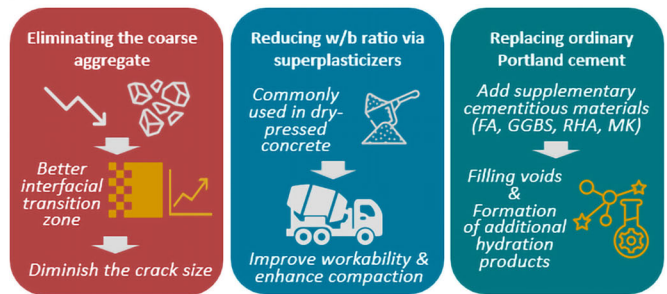


Fig. 2 | Fundamentals and approaches for improving the performance of fiber-reinforced UHPC. A Fiber/additives-related approaches; **B** Matrix-related approaches. To reduce the porosity and improve the microstructure of UHPC, optimal mixture proportion designs should be developed, including application of

fibers and mineral additives. To enhance homogeneity and optimize granular mixtures, approaches include eliminating the coarse aggregate, reducing the w/b ratio via superplasticizers, as well as replacing ordinary Portland cement with supplementary cementitious materials (SCMs).

fibers, steel fibers are regarded as the optimal choice for reinforcing UHPC, which exhibit exceptional stability under ambient temperature coupled with high Young’s modulus and tensile strength⁵³. Synthetic fibers, including PVA fiber, PP fiber, and PE fiber, exhibit lower tensile strength than steel fibers, thereby limiting their efficacy in enhancing tensile and compressive strength of UHPC⁵⁴. Nevertheless, they have the capability to enhance volume stability⁵⁵ and fire resistance⁵⁶ of UHPC. With the superior Young’s modulus and tensile strength, carbon fibers are able to enhance the mechanical characteristics of concrete while mitigating autogenous shrinkage⁵⁷. This improvement can be achieved with a minimal dosage of carbon fibers^{57–59}. The incorporation of 0.3 vol% carbon fibers resulted in a notable enhancement in the tensile strength and energy absorption capacity of UHPC in the existing study. Specifically, tensile strength of UHPC has increased 54.9 % from 5.87 MPa, along with an improvement of 108.9 % from 3.82 J regarding the energy absorption capacity⁵⁷. Detailed discussions on the effect of different fibers will be provided in Sections “Basic principles for improving performance” and “Influencing factors for fiber functionality”.

To enhance homogeneity and optimize granular mixtures, several methods should be considered which include eliminating the coarse aggregate, reducing the w/b ratio via superplasticizers, as well as replacing ordinary Portland cement with SCMs (e.g., fly ash (FA), ground granulated blast furnace slag (GGBS), rice husk ash (RHA), metakaolin (MK))^{60–62}. The mechanical and thermal characteristics of the cementitious matrix and aggregates in the conventional concrete are different, resulting in varying tensile and shear stresses within the interfacial transition zone (ITZ) and subsequently leading to microscopic cracks that are proportional to aggregate sizes^{1,63}. Therefore, reducing the size of aggregates in UHPC can diminish the crack size⁶⁴. This observation highlights an increase in the homogeneity of UHPC mixtures. Besides, the addition of SCMs contributes to the refinement of the UHPC microstructure by filling the voids between cement particles and acting as nucleation sites for the formation of additional hydration products⁶⁵. This leads to a denser and more compact

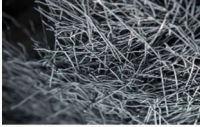

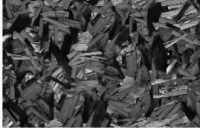


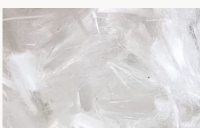
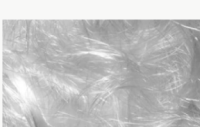
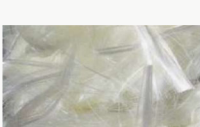

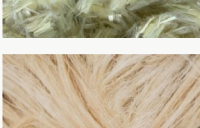
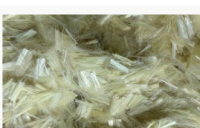
microstructure, resulting in improved mechanical properties. By reducing water demand, SCMs also enhance workability and cohesiveness, while their reaction with calcium hydroxide forms additional cementitious compounds, resulting in improved strength and durability^{60–62}.

Influencing factors for fiber functionality

As discussed above, the mechanical strength of UHPC can be improved by using fibers. These fibers bridge cracks and transfer stress between fiber and matrix, which capacity of fibers can be determined by bonding properties between fiber and matrix^{66–68}. The fiber/matrix bonding performance can be quantitatively determined by peak load measured in the single fiber pull-out test^{69,70}. During the pullout process, three resistance mechanisms are summarized that contains chemical adhesion, friction resistance, and mechanical anchorage, which is influenced by the diameter and shape of fibers^{71–73}. Specifically, the behavior of straight steel fibers during pullout can be divided into three stages: (1) initial load development without relative slip, (2) partial debonding resulting in a peak pullout load due to static friction and chemical adhesion, and (3) complete debonding and slip caused by dynamic friction. The pullout load decreases as displacement increases until complete separation, with friction resistance being the primary factor. Compared to straight fibers, hooked-end fibers exhibit an ongoing increase in pullout load by providing mechanical anchorage when passing through matrix. Consequently, mechanical anchorage and friction resistance emerge as two critical mechanisms that determine the pullout behavior of the hooked-end fibers^{74,75}. Regarding the inconsistent resistance mechanism of fibers with different shapes, bond strength of steel fibers can be categorized as follows: straight fibers exhibit the lowest bond strength at 6 MPa, while half-hook end fibers show a strength of 12.5 MPa, hook-end fibers demonstrate a range of 20.6 MPa to 23.5 MPa, corrugated fibers reach 33.3 MPa, and twisted fibers exhibit a strength range of 19.9 MPa to 47 MPa^{76,77}.

The bonding strength between fiber and matrix in UHPC is also influenced by the fiber embedding angle and the matrix curing method. To balance synergistic effect of snubbing, matrix spalling, as well as fiber slip

Table 1 | The characteristics of fibers employed in the advancement of UHPC properties

Fiber type	Steel fiber	Glass fiber	Carbon fiber	Basalt fiber	Polypropylene (PP) fiber	Polyethylene (PE) fiber	Polyester fiber	Polyvinyl alcohol (PVA) fiber	Nylon fiber	Cellulose fiber	Aramid fiber
Fiber photo											
Fiber diameter (μm)	100–1000	8–16	7–20	9–17	15–80	800–1000	10–80	1.1–1.5	20–30	24–400	10–15
Average density (g/cm ³)	7.85	2.74	1.7	2.7	0.91	0.95	1.3	1.35	1.17	1.4	1.44
Ultimate elongation (%)	Max 4 Min 0.5	3.5 2.5	1.6 1.2	3.15 3.0	28 15	5 3	15 10	50 5	20 15	NA	4.4 2.1
Tensile strength (MPa)	Max 2800 Min 280	2500 1400	4000 1800	2800 870	770 270	300 200	1200 650	850 770	960 900	1000 50	3200 2500
Young's modulus (GPa)	Max 250 Min 200	80 60	480 200	89 40	11 3.5	6 5	18 6	20 16	5 4	40 15	140 60

capacity, the maximum average bond strength was observed when an embedded angle ranging from 30° to 45° was employed^{78–80}. In addition, experimental observations revealed that under standard curing conditions, UHPC exhibited smooth fiber surfaces⁷⁶. However, in UHPC cured in autoclaves, residual cement paste adhered to the fiber surfaces, indicating an enhancement in chemical adhesion at fiber/matrix interface when UHPC cures under higher temperatures^{81–83}. For straight steel fibers, the bonding strength can be increased from 5.4 MPa to 14 MPa⁷⁶.

Optimizing the orientation and distribution of fibers can improve mechanical behavior of UHPC^{84–86}. The researchers have noted a 65% increase in bond strength when angle of fiber orientation angle varied from 0° to 45°, due to supplementary frictional shear resistance provided by the inclined filaments⁸⁷. By employing a 3D orientation analysis method utilizing X-ray CT techniques, researchers have established a robust linear correlation between the flexural strength of UHPC, the fiber orientation factor, and fiber quantities present at crack surfaces, which are closely tied to fiber distribution⁸⁸. Fiber orientation analysis allows estimation of degree of fiber alignment along tension direction; higher fiber orientation indicates more fibers aligned in tension direction. This alignment effectively restrains crack propagation, resulting in increased strength^{14,85,89}.

Synergistic effect for hybrid fibers

Different fiber types have different enhancement effects and mechanisms on the various properties of UHPC. Even if steel fibers are the most widely applied fibers, other types of fibers have also been extensively utilized in UHPC to address the limitations of steel fibers (i.e., the potential for corrosion, increased density leading to additional load, and higher costs)^{14,90–92}. Carbon-based additives are promising materials for reinforcing UHPC, which possess elastic modulus, excellent tensile strength and electrical conductivity^{93–95}. The commonly used carbon-based additives include carbon fiber, carbon nanotube (CNT), as well as graphite nanoplatelet^{57,58,96,97}. It has been proved that the enhanced connection between the fiber and matrix is facilitated by rough surface of carbon fibers⁹⁶. The utilization of CNT provides fiber bridging effects, filler effects, and nanoscale effects, thereby establishing the denser microstructure inside UHPC^{27,35,66}. In addition to carbon-based additives, synthetic fibers have also been shown to provide a significant increase in ductility of concrete. However, due to their hydrophobic nature, both PE fibers and PP fibers restrict the ingress of water into the internal spaces of the concrete matrix, consequently attracting more air bubbles to adhere to the fiber surfaces, thereby forming a porous ITZ^{98,99}. As a result, the mechanical properties of UHPC with the addition of synthetic fibers are lower than those of UHPC with the addition of steel fibers. PVA fibers exhibit hydrophilic characteristics and possess high chemical adhesion. However, within the UHPC matrix, their fracture becomes more severe as the strength of the surrounding matrix is sufficient to cause synthetic fiber breakage, thereby suppressing the increase in multiple cracking behavior and strain capacity¹⁰⁰. Additionally, poor dispersibility of synthetic fibers due to their high aspect ratio can lead to reduced workability, as longer fiber length may result in fiber agglomeration, leading to localized softening and the formation of weak zones¹⁰¹. Nevertheless, the addition of synthetic fibers can have beneficial effects on fire resistance, thereby enhancing the durability of UHPC. Pioneering studies have indicated that the incorporation of PP fibers can reduce the weight loss of UHPC exposed to temperatures exceeding 200 °C¹⁰². Simultaneously, the melting and expansion of synthetic fibers under elevated temperatures result in formation of micro-cracks and tunnels within the aggregate, thereby creating an interconnected network that significantly enhances the permeability of UHPC^{102,103}. This is an advantage not achievable with steel fibers. Furthermore, the utilization of mineral fibers (e.g., wollastonite and basalt fibers) not only enhances mechanical performance of UHPC but also offers the advantage of lower cost and corrosion resistance when compared to steel fibers. Basalt fibers are natural volcanic materials with a high melting temperature of 1450–1500 °C^{104,105}. Wollastonite fibers are natural silicate fibers containing SiO₂, CaO and Al₂O₃^{106,107}. Mineral fibers possess a similar constituent to

cementitious materials, helping to resist deformation of matrix and resulting in a stronger fiber/matrix bond^{105,108}. Furthermore, cellulose fibers which are natural polymer made from wood, were used as internal curing materials to limit shrinkage of UHPC^{109–111}. Cellulose fibers exhibit the advantages of abundant availability, ease of production, and substantial ecological value, while also serving to restrict width of crack and enhance durability of concrete¹¹². After presenting an overview of these fibers and their respective application effects, a crucial inquiry arises: can the simultaneous addition of these fibers along with steel fibers in UHPC result in advantageous synergistic enhancements?

The goal of incorporating hybrid fibers is to obtain synergistic effects of various fibers regarding the applications of UHPC^{113,114}. While in most studies, the substitution of steel fibers with hybrid fibers has shown limited improvement in compressive strength of UHPC, which it can even have a negative impact. However, the utilization of hybrid fibers can significantly enhance strain capacity and tensile strength of UHPC. Furthermore, utilization of hybrid fibers can have beneficial effects on the ductility¹¹⁵ and autogenous shrinkage^{116,117} of concrete. The application of hybrid fibers reduces propagation of micro-cracks within UHPC, resulting in decreased pore size and ultimately improving the microstructure of UHPC. Moreover, some studies have shown that the hybrid utilization of steel fibers and PP fibers in concrete exhibits the synergistic effect on crack initiation, which mechanism behind involves the integration of the pull-out behavior of steel fiber and disruptions caused by PP fibers¹¹⁸. Additionally, chloride ion permeability of UHPC can be significantly reduced by this type of combination (i.e. steel fibers and PP fibers), which reduced the sensitivity of UHPC to corrosive environments¹¹⁹. These findings suggest that using hybrid fibers holds promising potential for improving the durability and sustainability of UHPC.

Research progress in multiscale mechanics

Multiscale characteristics of UHPC. UHPC, as a representative heterogeneous material, exhibits distinctive multi-scale structural characteristics. Its constituents primarily encompass cement, fly ash, blast furnace slag, silica powder, water, fine aggregates and additives. In particular, to enhance the sustainability of UHPC, the global academic community is concerned with reducing the use of cement without compromising its performance. The incorporation of nanomaterials as additives in cementitious materials has emerged as a popular approach to address this challenge. When extending investigation from macro scale to micro scale, the crystal core effect and electrical properties of materials surface is continuously changing, thereby giving rise to novel properties such as the micro-size effect and surface-related phenomena that remain unattainable at macro scale. By capitalizing on the unique attributes exhibited by nanomaterials, it becomes possible to manipulate the hydration process of cement, subsequently influencing the mechanical properties and long-term durability of the hardened paste^{120–122}. Hence, nanoadditives can be a substitute for cement in UHPC, reducing CO₂ emissions and improving its performance, and they can even add new properties. In this case, UHPC exhibits both compositional heterogeneity and spatial discontinuity, possessing discrete characteristics at the nanoscale (i.e., spatial discontinuity) as well as compositional heterogeneity. At the microscale and mesoscale, due to the incorporation of a significant amount of ultrafine cementitious materials and the utilization of the low w/b ratio, UHPC typically exhibits a denser microstructure compared to ordinary concrete^{123,124}. The crucial constituents in the microstructure of UHPC encompass quartz powder, hydration materials (e.g., gelatinous calcium silicate hydrate gel), and unhydrated cement clinker. These components hold significant relevance in the meticulous assessment of UHPC's microstructural characteristics. Compared to conventional concrete, ITZ in UHPC is less porous, lighter and significantly denser, as maximum calcium hydroxide crystals are converted into thick hydrated calcium silicate (C-S-H) gels due to low w/b ratio and pozzolanic reactions between calcium hydroxide and reaction admixtures^{98,99,125}. With its distinctive microstructure, UHPC

demonstrates an innovative composition resulting from the enhanced ITZ and the tightly packed arrangement of solid particles. Therefore, the investigation of the mechanical properties of UHPC requires additional effort to take into account its unique material characteristics.

Due to the complementary and synergistic effects achievable by incorporating different types of fibers, hybrid fiber-reinforced UHPC represents a cutting-edge direction regarding its advancement¹²⁶. Currently, research on hybrid fibers in terms of fiber selection and understanding their reinforcement mechanisms heavily relies on empirical experimentation, leading to resource wastage and a lack of systematicity in studies related to hybrid fiber-reinforced UHPC^{127,128}. Therefore, a multi-scale analysis is necessary to thoroughly investigate the mechanisms of performance enhancement and cross-effects of different fibers in concrete. Through simulations and experimental data, based on parameters such as strength, stiffness, and fiber reinforcement at various scales, it is essential to establish a comprehensive and systematic fiber matching principle^{129,130}. This will provide a solid foundation for fiber selection in hybrid fiber-reinforced UHPC, reducing resource wastage and offering theoretical support and research methods for the development of novel high-performance UHPC.

Multiscale theoretical methods. The comprehensive study of multi-scale mechanics of UHPC requires a holistic consideration of its structural characteristics at macroscopic, mesoscopic, and microscopic scales^{63,131–133}. By employing multi-scale analysis methods, it is crucial to investigate the relationships between the compositional distribution, micro-nano features, and mechanical properties of UHPC. It aims to establish quantitative relationships between the macroscopic performance of cementitious composites and the properties of their constituent materials, as well as the various structural characteristics at different scales. Furthermore, it seeks to elucidate the underlying mechanisms by which different organizational forms at each scale contribute to the disparate macroscopic performance exhibited by the materials²⁰.

Regarding the multiscale analysis of concrete, the approaches principally encompass two distinct methodologies: hierarchical and concurrent methods. Table 2 presents a compilation of commonly employed theoretical and simulation methods in multi-scale analysis^{134–136}. Hierarchical methods decompose the practical problem into multiple levels based on different temporal or spatial scales¹³⁷. Subsequently, appropriate parameters are selected to forge connections across these disparate levels. The analysis can either proceed from microscopic to macroscopic properties through a step-by-step equivalence and inversion or optimize the material's structure from macroscopic requirements, employing theoretical or numerical methods to link performance across scales¹³⁸. Effective use of hierarchical approaches demands a deep understanding of the analysis process and material properties to choose key parameters accurately and ensure analysis precision. Concurrent method simultaneously addresses multiple scales in a single experiment¹³⁹. It integrates mesoscopic, microscopic, and nanoscale regions within a continuum model's computational domain, using mathematical relationships for scale coupling^{140,141}. Typically employing a continuum model, it resorts to molecular or quantum mechanics models for critical areas like crack tips. This method facilitates parallel multiscale computation, reducing complexity while preserving accuracy^{142,143}, aiming for achieving universally applicable full-scale simulations panning the nanoscale, microscale, mesoscale, and macroscale^{144,145}. Concurrent methods are primarily applicable to numerical simulations, which will be further discussed in Section "Multiscale modeling methods". To date, the authors' review reveals an absence of any unified mechanical theories that adequately span all length scales required for concurrent multiscale analysis.

For heterogeneous composite materials such as UHPC, resolving the interfaces between distinct components is a critical aspect of hierarchical theoretical approaches, aimed at enhancing the understanding of their mechanical responses under load, the transfer of load between components, and the resultant alterations in material structure. Among these, the cohesive zone model (CZM) stands as one of the frequently utilized methodologies for analyzing load transfer issues at the interfaces of concrete and other

Table 2 | Overview of the recent progress in the theoretical, simulation and experimental approaches of multiscale mechanics

Experimental approaches		Theoretical approaches		Simulation approaches		
Method	Apparatus	Characterization parameters	Hierarchical	Concurrent	Hierarchical	
Macro-scale (m~mm)	Strain sensor; Electronic speckle pattern interferometry (ESPI); High-speed camera ...	Modulus, Stress, strain, Bending stiffness, Strength ...	Cohesive zone model; Shear-lag methods; Voigt-Reuss-Hill (VRH) approximation; Hashin-Shtrikman (HS) bounds; Mori-Tanaka method; Sparse methods; Self-consistent method; Differential method; interaction direct derivative (IDD) method; ...	The current knowledge of the authors has not yet acknowledged any unified mechanical theories that can encompass all-length scales for concurrent multiscale analysis.	Finite element method (FEM); Extended finite element method (XFEM); Boundary element method (BEM); Finite volume method (FVM); Discrete element method (DEM); Meshless method; Cell-based method; Voronoi cell finite element method (VCFEM) ...	Concurrent
Micro-scale (µm~mm)	Fiber tensile tester; Laser profilometer; X-ray diffraction instrument (XRD); Computed tomography (CT); Optical microscope (OM); Scanning electron microscope (SEM) ...	Porosity; Cracks; Damage; Elongation; Material micro-structure ...			Surface Antenna Array Decoupling (MAAD) method; Continuum-molecular dynamics overlap method; Micro-nano molecular dynamics method (MIMMD);	
Meso-and nano-scale (nm ~ µm)	Nanoindentation; Transmission electron microscope (TEM); Scanning electron microscope (SEM); Scanning tunneling microscope (STM); Atomic force microscope (AFM) ...	Modulus; Strength; Fracture toughness; Interfacial adhesion energy; Interfacial shear strength ...	Cauchy-born rule; Nonlocal theory ...		Density functional theory (DFT); Ab initio molecular dynamics (AIMD); Molecular dynamics (MD); Monte Carlo simulation (MC); Peridynamics (PD); Coarse-grained (CG) modeling; Cluster statistical thermodynamics (CST); Generalized homogenization (GMH) ...	Quasi-continuum method (QC); Hybrid molecular/cluster statistical thermodynamics method (HMST); Heterogeneous multiscale method (HMM) ...

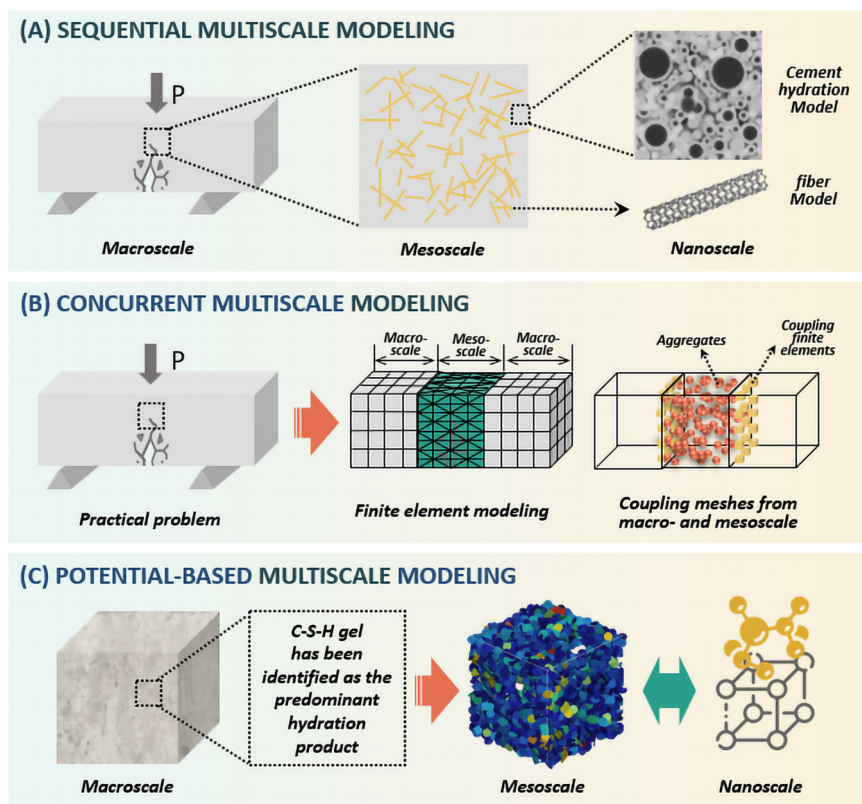
composite materials. With CZM, localized damage in materials can be effectively captured and modeled through nonlinear springs that denotes the major physical variables. CZM surpasses linear elastic fracture mechanics by incorporating microscale details and the fracture processing zone, thus enabling a comprehensive analysis of failure mechanisms and energy dissipation. Moreover, CZM integrates crack initiation and growth into a unified framework, facilitating its straightforward formulation and application in numerical simulations. CZM stands out among models addressing concrete fractures, primarily due to its optimal balance between conceptual simplicity, computational ease, and predictive precision.

Recently, CZM has experienced considerable advancement in its application. CZM can be applied to simulate the fiber reinforced polymer (FRP)-concrete interface debonding under different loading conditions (e.g. mix-mode)^{146,147}. Utilizing a mode-independent traction-separation law, the shear and peel responses of interface can be modeled. Analytical expressions for normal and shear stresses at the interface, as well as axial load of FRP plate, are derived for various stages of debonding, thereby integrating initiation and progression of debonding into a singular framework. CZM can also be applied to coupling with thermal flux-separation relation and diffusion flux-separation relation in multiscale modeling, enabling the prediction of temperature and humidity jump across cohesive cracks¹⁴⁸. In this model, the meso-structure of concrete is characterized by randomly distributed aggregates embedded within the cement paste, complemented by zero-thickness interface elements that represent ITZ between cement and aggregates. CZM is applied to model the debonding at the ITZ. Additionally, the development of the mixed-mode CZM is grounded in strength models rather than traction laws¹⁴⁹. It facilitates the independent choice of models for each direction, offering benefits for simulations under mixed-mode conditions and highlighting constraints in approaches reliant on effective displacements. With this advancement, the traction-separation law and or strength model¹⁵⁰ in CZM can be combined with micromechanically motivated thermal and diffusion flux-separation relation to accurately describe ITZ between cement and aggregates on concrete's mechanical, thermal, and diffusion characteristics.

Multiscale modeling methods. UHPC exhibits complex compositions and its material interior possesses discontinuous spatial distribution, showcasing typical characteristics of a discrete body¹⁵¹. Notably, in UHPC with the addition of reinforcing phases, the material remains discontinuous at the nanoscale, and the interactions between atoms exhibit significant nonlinearity¹⁵². Therefore, the inclusion of nanoscale analysis is necessary within the multi-scale framework. This entails establishing a relationship between the interactions among atoms and the parameters of the continuum medium¹⁵³. Simulation methods that encompass atomic and quantum scales, such as first-principles and MD simulations, offer precise modeling of atomic and quantum phenomena¹⁵⁴. Yet, due to computational limitations, the capacities of these atomistic scale methods fall significantly short of the requirements for simulating practical problems^{155,156}. Therefore, multiscale simulations have emerged as the primary approach to address the coupling problems between the nanoscale and macroscopic scales. As shown in Fig. 3, currently the multi-scale simulation approaches involving discrete bodies can be categorized into the following categories:

The first approach is the sequential multiscale modeling, includes decoupling the scales and employing corresponding methods for analysis at each scale sequentially^{29,97}. In atomistic scale, the atomic configuration and interatomic interactions are monitored through first principles and MD simulations^{66-68,157}. The mesoscale modeling requires the information obtained from representative volume elements (RVE) that applied equivalent properties from the atomistic results. Then, through finite element and continuum simulation methods, macroscopic constitutive relationships are established. These relationships are subsequently applied to address practical problems. For instance, in the investigation of the mechanical properties and fracture behavior of CNT-reinforced concrete, at least three scales are defined^{158,159}. MD simulation is applied to simulate the

Fig. 3 | Systematic diagram of multiscale modeling methods in UHPC. A Sequential multiscale modeling: how to investigate the mechanical properties and fracture behavior of fiber-reinforced concrete¹⁵⁸; B Concurrent multiscale modeling: how the handshake coupling method could be applied to the crack predicting for concrete¹⁷⁶; C Potential-based multiscale modeling: example of coarse-grained cementitious materials⁹⁷.



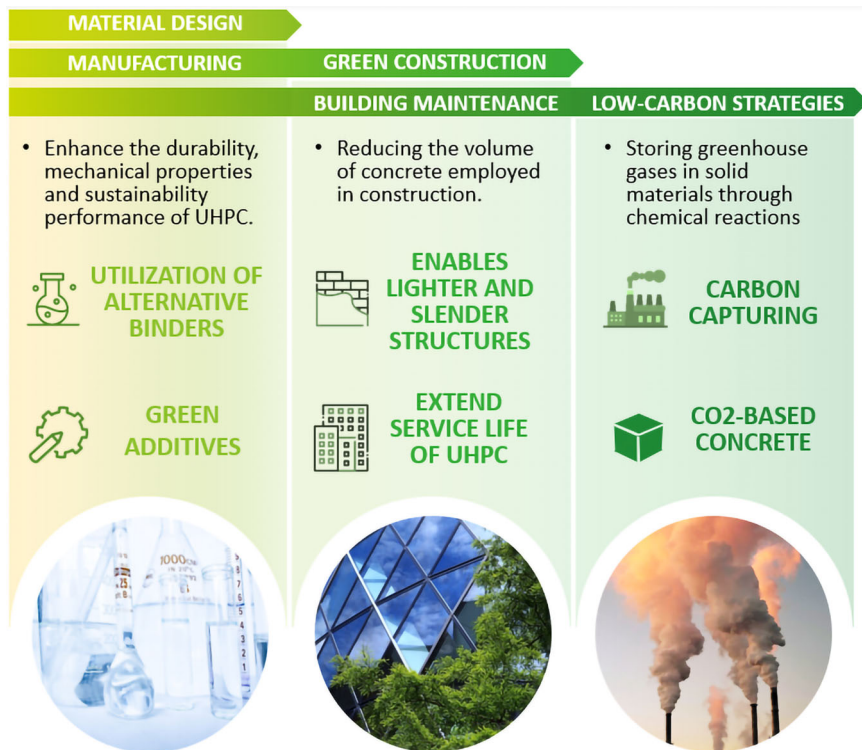
tensile behavior of CNT at the nanoscale, from its mechanical properties that are scaled up to the microscale. Then, a hydration model determines the chemical composition of cement, leading to the construction of RVE based on hydration results. Subsequently, FEM assuming isotropic damage across all phases, assesses the mechanical and damage characteristics of bulk material. This microscale homogenized response is then elevated to the macroscale using the extended finite element method (XFEM) for damage analysis, aiming to forecast damage patterns in three-point bending tests and mixed-mode crack growth. This case study also illustrates that the complexity of multiscale analysis renders real-time coupling techniques a challenge within the framework of sequential multiscale modeling¹⁶⁰. It also underscores that possessing a deep and comprehensive understanding of mechanical processes is crucial for selecting key parameters, so as to enhance the accuracy and efficiency of modeling¹⁶¹.

The second approach is the concurrent multiscale simulation method that directly couples atomistic simulations with continuum simulations¹⁶². In multi-scale simulations that combine atomistic simulations with finite element methods, the computational domain is typically divided into a continuum region, an atomistic region, and a transitional region. The key to successful cross-scale simulation lies in effectively handling the interface or transitional region between the continuum and atomistic domains. A more direct approach to address this is by gradually refining the finite element mesh in the transitional region to the scale of atomic lattice. At the interface, the mesh nodes are directly associated with individual atoms, maintaining a one-to-one correspondence at the interface between two scales throughout the deformation process¹⁶³. This method is referred to as the interface coupling method. Currently, commonly used interface coupling methods include the Finite-Element combined with Atomistic modeling (FEAt) method¹⁶⁴, the coupled atomistic and discrete dislocation (CADD) method^{165,166}, the Meta-Surface Antenna Array Decoupling (MAAD) method^{167,168}, and the AFEM/FEM method^{16,169–171}. However, in interface coupling methods, reducing the finite element mesh size in the transitional region to the scale of atomic lattice poses modeling challenges and may introduce computational errors. Therefore, other coupling multi-scale

methods have been proposed referred to as handshake coupling methods. In handshake coupling methods, when dealing with the transitional region (or coupling region), the finite element mesh nodes are no longer directly tied to individual atoms. Instead, macroscopic mechanical quantities and microscopic mechanical quantities are related through averaging, superposition, and other methods. Currently, the main weak coupling methods include the continuum-molecular dynamics overlap method¹⁷², the bridging scale method (BSM)¹⁷³, the bridging domain method (BDM)¹⁷⁴, and the micro-macro molecular dynamics method (MMMD)¹⁷⁵. For instance, the handshake coupling method could be applied to the crack prediction for concrete¹⁷⁶. In elastic regions of concrete, a macroscopic model utilizing uniform elastic parameters is employed. For zones anticipated to develop cracks, a mesoscopic approach employing mesh fragmentation considers concrete as a diverse three-phase material, including mortar matrix, coarse aggregates, and ITZ. Then, coupling finite elements are applied for coupling non-matching meshes between macro and mesoscale. The crack initiation and propagation process in concrete is monitored through the mesh fragmentation technique.

The third category of methods is the multi-scale approach based on interatomic potential functions, which couples the concepts of discrete bodies and continua by utilizing potential energy functions^{140,141}. This approach enables multi-scale simulations within a unified algorithmic framework¹⁷⁷. Among them, typical representative methods include the quasi-continuum method (QC)¹⁷⁸, coarse-grained (CG) modeling^{97,143,179}, and molecular statistical thermodynamics (MST)¹⁸⁰. For cementitious materials, some pioneering studies have developed CG models. Among those, C-S-H gel has been identified as the predominant hydration product, constituting over 50% of the volume fraction and serving as the primary binding agent in cement matrices¹⁸¹. It has been extensively adopted in MD simulations and CG models for studying cement-based composites^{182,183}. C-S-H particles are utilized to simulate CNT-reinforced cementitious composites, modeled as polydisperse spherical particles with interactions governed by a modified Lennard-Jones potential^{97,184}. These models involve grid partitioning of the computational domain and derive motion equations

Fig. 4 | Overview of the strategies to enhance the sustainability and environmental friendliness of UHPC. The framework commences with sustainable design, highlighting the utilization of alternative binders and green additives. Subsequently, it transitions to green construction techniques, illustrating UHPC's role in fostering sustainable progress in structural endeavors. The depiction culminates with an overview of pioneering low-carbon approaches, signifying a forward-looking commitment to reducing the carbon footprint in UHPC.



from molecular dynamics equations of motion. Additionally, they derive mass and stiffness matrices from interatomic potential functions and establish constitutive relationships that are specific to the grid size. The entire computational domain lacks an interface between the continuum and atomic systems, enabling seamless connection across different scales. Compared to the quasi-continuum method, CG modeling can account for a larger-range of temperatures and is suitable for studying dynamic phenomena such as material fracture, interfacial debonding mechanism and crack propagation¹⁸⁵.

Ecological considerations in practical applications. The greenhouse effect is a major global environmental concern, poses a critical challenge to achieving sustainable development in the modern era. Previous research has indicated that cement production contributes approximately 5% of the overall carbon dioxide emissions¹⁸⁶. The significant responsibility of the construction industry to reduce emissions arises from the high emission rate associated with concrete. Consequently, it is critical to make significant progress in terms of ecological and sustainable development in material manufacturing, green construction, and building maintenance¹⁸⁷. Here we present the overview of the strategies to enhance the sustainability and environmental friendliness of UHPC in Fig. 4. While UHPC typically exhibits higher cement content compared to conventional concrete that releases more energy-related CO₂¹³, it allows for the design of thin and lightweight structures^{188,189}. This, in turn, leads to a reduction in the amount of concrete used during construction and decreases emissions associated with material transportation. Moreover, numerous studies have been conducted to reduce the cement content of UHPC without compromising its performance. Additionally, sustainable UHPC is capable of withstanding harsh environments that can effectively reduce carbon emissions in building maintenance, making it an effective approach to enhancing building sustainability¹⁹⁰.

Sustainable design

To enhance the sustainability performance of UHPC, the utilization of alternative binders and green additives and proves to be an effective

approach. Based on carbon footprint assessment, the developed eco-UHPC that incorporates dehydrated cementitious powder (DCP) in the matrix can be regarded as a sustainable and environmentally friendly product. From a sustainability perspective, increasing the dosage of DCP is beneficial to further improve UHPC performance¹⁹⁰. It has been indicated that CO₂ emissions from per unit of sustainable UHPC and the ratio of CO₂ emissions/compressive strength decrease with the increase of DCP content¹⁹¹, which shows that green UHPC exhibits better utilization of cement. Moreover, the CO₂ emissions during UHPC production also can be greatly decreased with the addition of DCP¹⁹². According to measurements, a conventional UHPC composed solely of pure cement necessitates 377 kg of CO₂ per unit volume. With a 25% increase in DCP content, the emissions can be reduced to 298 kg, which reduces 21% of the initial CO₂ emission¹⁹¹.

The utilization of green additives, such as by-products from the power sector like fly ash, enables UHPC to further advance towards sustainable development by incorporating materials that would otherwise be discarded. Several solid waste resources can serve as substitutes and have been incorporated into concrete and mortar to enhance their properties and conserve energy, including construction and demolition waste^{193,194}, fly ash²¹, metakaolin¹⁹⁵, silica fume¹⁹⁶, waste glass^{47,48,197}, plastic waste¹⁹⁸, marble waste¹⁹⁹ and rock waste²⁰⁰. However, it has been reported that the utilization of green additives in UHPC concrete may possess a negative effect on fresh and mechanical properties, necessitating early consideration in roadways and structural applications to ensure optimal performance⁶⁵.

Evaluating the effectiveness of alternative binders and additives involves assessing their impact on UHPC's mechanical properties, environmental benefits, economic viability, chemical and physical compatibility, and compliance with regulatory standards. Materials such as fly ash, silica fume, ground granulated blast furnace slag, and rice husk ash have shown promise in enhancing UHPC's performance, offering improved compressive strength, durability, and workability. The sustainable design of UHPC using waste materials not only addresses the environmental impact of construction by reducing CO₂ emissions and virgin raw material consumption but also contributes to waste reduction. The challenge lies in balancing performance, sustainability, and cost, necessitating ongoing

research to optimize the formulation of UHPC with waste materials for a greener construction industry. Currently, the selection of alternative binders and additives for UHPC remains limited and relies primarily on experimental and empirical approaches. The lack of mechanistic understanding hinders the determination of optimal additive proportions. Thus, it is crucial to employ a multiscale mechanics approach for establishing quantifiable correlations between the categorization of UHPC compositions, additive content, and macroscopic performance²⁰¹.

Green construction. The enhanced mechanical strength of UHPC enables the construction of lighter and slender structures, consequently reducing the volume of concrete employed in construction^{13,202}. Specifically, the exceptional strength of UHPC enables the construction of slender structures, resulting in a reduction in the self-weight of the structures. UHPC structural elements with reduced cross-sectional dimensions also free up valuable architectural space¹⁸. Moreover, with its exceptional strength-to-unit weight ratio, low permeability, and compact microstructure, UHPC showcases excellent resistance to both fire and explosive spalling at elevated temperatures^{71,102,105,108,203}. These superior properties extend the length of service life of UHPC significantly, leading to a reduction in demolition waste, transportation demands, and environmental pressures.

Regarding materials, the microstructural and macroscopic characteristics of UHPC mixtures have been investigated, aiming to enhance these properties by substituting valuable, limited, or unavailable traditional components to achieve maximum practical density^{96,99}. UHPC combines the advantages of fiber-reinforced concrete, high-strength concrete and self-compaction concrete⁴¹. The compressive strength is measured at 150 MPa, coupling with flexural and tensile strength of 30 MPa and 5 MPa respectively. It is estimated that replacing ordinary concrete with UHPC can reduce the total aggregate content (including fine and coarse particles) used in structural components by 30%. The 100% proportion of coarse aggregates can be reduced⁹⁶, resulting in a reduction in the consumption of concrete raw materials.

Regarding structural application, the environmental benefits of UHPC have been confirmed through practical case studies in the construction industry. An evaluation is conducted to assess the energy consumption and life cost of a bridge design that incorporates both timber and UHPC²⁰⁴. The UHPC components used in the bridge deck require negligible maintenance over 100 years or more. This extended maintenance-free lifespan, coupled with reduced maintenance work and the use of fewer materials in the design, contributes to an exceptionally low annual CO₂ emission. It is also reported that three distinct UHPC bridges were constructed in diverse locations for comparison²⁰⁵. Comparisons have been made between the greenhouse gas emissions of highway bridges constructed using UHPC and those of standard concrete highway bridges²⁰⁶. It was observed that when considering only concrete emissions, the CO₂ emissions were reduced by 50%²⁰⁵. A study has been conducted to model the repair of highway bridges, which includes three different repair material systems: traditional concrete (using waterproof membrane), UHPC, and eco-UHPC²⁰⁷. Regarding eco-UHPC system, the environmental impact of cement is notably diminished compared to UHPC system, achieved through the substitution of 50% of cement with limestone filler. Negative environmental impact of repair solutions with both UHPC and eco-UHPC is significantly lower compared to that of standard solutions, which enable reductions of 60% and 72%, respectively²⁰⁷. Global warming potential has decreased 42% in comparison with eco-UHPC with the typical UHPC mixture²⁰⁷. These studies demonstrate carbon footprint and cost-effectiveness of using UHPC have significantly improved the ecological benefits of construction²⁰⁷, also showing the potential of UHPC and promoting its widespread use to mitigate environmental impacts¹³.

Low-carbon strategies. Carbon capturing is a technology that stores greenhouse gases in solid materials through chemical reactions. It addresses climate change by reducing emissions and utilizing the

advantages of ecological raw materials, while creating commercially viable and sustainable products^{13,208}. CO₂-based concrete provides an alternative and ecological approach for carbon capturing. Concrete has the capacity to accommodate the CO₂ generated by cement production facilities. Concrete can undergo carbonation, capturing CO₂ through the rapid carbonation of its constituent minerals, carbonation during hydration, and the overall carbon capturing process. The collected CO₂ from cement manufacturers can be pumped into UHPC, facilitating a reaction with calcium-rich hydration products such as C-S-H and calcium hydroxide to produce calcium carbonate (CaCO₃)²⁰⁹. The exceptional durability of UHPC manifests in its resistance to carbonation, corrosion, and transport capacity, contributing to the formation of a dense and uniform matrix characterized by an extraordinarily low porosity. The significantly low permeability and lower water-to-cement ratio endow UHPC with remarkable resistance to carbonation¹⁸⁸. The results of the rapid chloride permeability test (RCPT) conducted on UHPC specimens are consistent with the findings of the surface resistivity test, demonstrating a significantly high energy passing range of 3000–10,000 Coulombs across various non-proprietary mixtures²¹⁰.

However, carbon capturing technology for UHPC still faces challenges. It is reported that the compressive strength of carbon capture concrete (CCU) can be reduced through CO₂ curing²¹¹. Under such circumstances, CCU requires a higher ordinary Portland cement content to attain comparable compressive strength as conventional concrete. The carbon emissions from the production of ordinary Portland cement play a notable role in terms of CO₂ output. Heightening the ordinary Portland cement proportion in concrete mixtures leads to amplified CO₂ emissions during the upstream cement manufacturing process, potentially nullifying the advantages derived from CO₂ capture and utilization in concrete production. Therefore, during the development of carbon capturing technologies, conducting a multiscale pre-assessment of carbon capture in UHPC can aid in identifying the most effective research strategies to address the issue of greenhouse gases.

Challenges and perspectives. Despite the exceptional mechanical and durability properties of UHPC, which enhance its application in resilient and sustainable reinforced concrete structures²¹², its widespread deployment still faces certain challenges. In terms of the design for sustainable UHPC, the substitution of cement with alternative binder materials (e.g., fly ash, slag, and silica fume) poses challenges in achieving early-age mechanical performance in UHPC. As coal-fired power plants shift towards natural gas plants, traditional supply chain management becomes increasingly limited. Hence, further research is also required to explore sustainable SCMs¹⁴. For UHPC with added nano-additives, achieving a uniform dispersion of nanomaterials within the concrete matrix remains challenging. Consequently, the proportion of nanoparticles substituting cement in UHPC remains relatively low. Further research is needed to explore the dispersion of nanomaterials and maintain their effectiveness at higher dosages in UHPC¹²⁰. This can be achieved through the application of multiscale mechanical analysis methods. Furthermore, the mechanism behind the seeding effect, which constitutes a fundamental role of nanomaterials in UHPC, remains unclear. Employing finite element techniques can shed light on this phenomenon. Consequently, there is a need for additional research to explore the impact of varying nanomaterial sizes on the performance of UHPC¹²⁰.

The production aspect of UHPC materials is equally confronted with challenges. Due to its elevated packing density and absence of coarse aggregate, UHPC exhibits a higher homogeneity compared to conventional concrete as its higher packing density and without coarse aggregate which also causes straight-line cracks. Enhancing the ductility and tensile strength of UHPC can be achieved through the incorporation of fibers that effectively impede crack propagation²¹³. However, the low w/b ratio, addition of fibers, and reduced workability of UHPC lead to challenges during the casting process of UHPC. Moreover, the orientation, distribution, and type of fibers

have an impact on the macroscopic properties of UHPC^{84,86}. Therefore, the casting of slender UHPC elements still requires an effective method to ensure the proper distribution and orientation of fibers within the cementitious matrix. Additionally, high-energy mixers are necessary for processing UHPC due to its low w/b ratio¹⁷.

Numerous challenges are also encountered in the practical applications of UHPC. UHPC constructions present deviations from conventional reinforced concrete practices, necessitating a proficient workforce comprising builders, engineers, and specialists who possess expertise in UHPC technology and design considerations. However, the availability of qualified personnel in this domain remains limited, emphasizing the need for teams well-versed in UHPC methodologies and design intricacies⁴¹. In the establishment of regulations within the construction industry, it is crucial to develop fair and accurate strategies for the optimization of UHPC components and mix designs. Relying solely on experimental blends is insufficient, necessitating the utilization of multiscale analytical methods³⁰. In the formulation of UHPC design and construction criteria, a comprehensive approach that incorporates field experience, empirical analysis, and scientific calculations is vital. The complexities of establishing international guidelines arise from the diverse experiences with UHPC across different countries⁴¹. Efforts have been made by China, France, Germany, Japan, and Switzerland to standardize UHPC, aiming to facilitate its widespread adoption. France took a significant step in 2016 by announcing its inaugural UHPC standard²¹⁴.

Despite facing challenges, UHPC has undergone several decades of development and continues to be a promising and sustainable construction material. As discussed extensively in Section “Fundamentals of Fiber-reinforced UHPC”, the rapid advancements in multiscale mechanics hold great potential for invigorating the material design of UHPC. Meanwhile, the integration of AI with construction materials and the Industry 4.0 framework can also achieve the intelligent design and application of UHPC²¹⁵. This innovation process integration process is based on computer science, starting from the digitization of building materials, developing towards advanced manufacturing, and ultimately reaching the level of intelligent application and operation of UHPC buildings^{216,217}. Nowadays, innovative work in additive manufacturing (3D printing) provides promising technologies for various fields including UHPC^{218,219}. In principle, the use of a printing machine for concrete extrusion offers a straightforward and expeditious approach to constructing intricate three-dimensional structures^{220,221}. Several recent studies have demonstrated the feasibility of using UHPC in 3D printing^{222–224}, indicating that 3D printing developed using UHPC-related materials has better shape retention than using traditional cast UHPC. However, there is still a lack of implementation records for 3D printing based on UHPC projects, due to technical limitations in 3D printing process and configuration (i.e., pumping rules, addition of fibers, flow rate, and nozzle design)²²⁵. Although there have been cases of UHPC 3D-related printing, current attempts are limited to low-complexity 3D printing. Present investigations call for the design and fabrication of 3D-printed UHPC materials endowed with pumpability, constructability, and extrusion capabilities, thus highlighting the remarkable prospects in the development of UHPC 3D printing technology²²⁶.

Received: 30 December 2023; Accepted: 8 March 2024;

Published online: 10 June 2024

References

- Zhou, A., Büyükoztürk, O. & Lau, D. Debonding of concrete-epoxy interface under the coupled effect of moisture and sustained load. *Cem. Concr. Compos.* **80**, 287–297 (2017).
- Zhou, A., Chow, C. L. & Lau, D. Structural behavior of GFRP reinforced concrete columns under the influence of chloride at casting and service stages. *Compos. B Eng.* **136**, 1–9 (2018).
- Zhou, A. et al. Understanding the Toughening Mechanism of Silane Coupling Agents in the Interfacial Bonding in Steel Fiber-Reinforced Cementitious Composites. *ACS Appl. Mater Interfaces* **12**, 44163–44171 (2020).
- Richard, P. & Cheyrezy, M. Composition of reactive powder concretes. *Cem. Concr. Res.* **25**, 1501–1511 (1995).
- Shao, Y., Tich, K. L., Boaro, S. B. & Billington, S. L. Impact of fiber distribution and cyclic loading on the bond behavior of steel-reinforced UHPC. *Cem. Concr. Compos.* **126**, 104338 (2022).
- Li, W. et al. Comparative study of compressive behavior of confined NSC and UHPC/UHPFRC cylinders externally wrapped with CFRP jacket. *Eng. Struct.* **292**, 116513 (2023).
- Li, W., Lu, Y., Shi, T. & Wang, P. A novel double bridging-slipping (DBS) concept to overcome deformation incompatibility of textile reinforced-engineering cementitious composite (TR-ECC). *Case Stud. Constr. Mater.* **19**, e02475 (2023).
- Li, J., Wu, Z., Shi, C., Yuan, Q. & Zhang, Z. Durability of ultra-high performance concrete – A review. *Constr. Build Mater.* **255**, 119296 (2020).
- Valcuende, M., Lliso-Ferrando, J. R., Ramón-Zamora, J. E. & Soto, J. Corrosion resistance of ultra-high performance fibre-reinforced concrete. *Constr. Build Mater.* **306**, 124914 (2021).
- Sohail, M. G., Kahraman, R., Al Nuaimi, N., Gencturk, B. & Alnahhal, W. Durability characteristics of high and ultra-high performance concretes. *J. Build. Eng.* **33**, 101669 (2021).
- Cui, K., Liang, K., Chang, J. & Lau, D. Investigation of the macro performance, mechanism, and durability of multiscale steel fiber reinforced low-carbon ecological UHPC. *Constr. Build Mater.* **327**, 126921 (2022).
- Arora, A., Almujaiddi, A., Kianmofrad, F., Mobasher, B. & Neithalath, N. Material design of economical ultra-high performance concrete (UHPC) and evaluation of their properties. *Cem. Concr. Compos.* **104**, 103346 (2019).
- Randl, N., Steiner, T., Ofner, S., Baumgartner, E. & Mészöly, T. Development of UHPC mixtures from an ecological point of view. *Constr. Build Mater.* **67**, 373–378 (2014).
- Du, J. et al. New development of ultra-high-performance concrete (UHPC). *Compos. B Eng.* **224**, 109220 (2021).
- Nilimaa, J. Smart materials and technologies for sustainable concrete construction. *Dev. Built Environ.* **15**, 100177 (2023).
- Wang, P., Ke, L., Wu, H., Leung, C. K. Y. & Li, W. Hygrothermal aging effects on the diffusion-degradation process of GFRP composite: Experimental study and numerical simulation. *Constr. Build Mater.* **379**, 131075 (2023).
- Akhnouk, A. K. & Buckhalter, C. Ultra-high-performance concrete: Constituents, mechanical properties, applications and current challenges. *Case Stud. Constr. Mater.* **15**, e00559 (2021).
- Sritharan, S. Design of UHPC structural members: Lessons learned and ASTM test requirements. *Adv. Civ. Eng. Mater.* **4**, 113–131 (2015).
- Amran, M., Murali, G., Makul, N., Tang, W. C. & Eid Alluqmani, A. Sustainable development of eco-friendly ultra-high performance concrete (UHPC): Cost, carbon emission, and structural ductility. *Constr. Build Mater.* **398**, 132477 (2023).
- Wang, X. Q., Chow, C. L. & Lau, D. A Review on Modeling Techniques of Cementitious Materials under Different Length Scales: Development and Future Prospects. *Adv. Theory Simul.* **2**, 1–15 (2019).
- Liang, K., Wang, X. Q., Chow, C. L. & Lau, D. A review of geopolymer and its adsorption capacity with molecular insights: A promising adsorbent of heavy metal ions. *J. Environ. Manage.* **322**, 116066 (2022).
- Zhou, A., Tam, L. H., Yu, Z. & Lau, D. Effect of moisture on the mechanical properties of CFRP-wood composite: An experimental and atomistic investigation. *Compos. B Eng.* **71**, 63–73 (2015).
- Kai, M. F., Zhang, L. W. & Liew, K. M. Carbon nanotube-geopolymer nanocomposites: A molecular dynamics study of the influence of

- interfacial chemical bonding upon the structural and mechanical properties. *Carbon N. Y.* **161**, 772–783 (2020).
24. Kai, M. F., Zhang, L. W. & Liew, K. M. Graphene and graphene oxide in calcium silicate hydrates: Chemical reactions, mechanical behavior and interfacial sliding. *Carbon N. Y.* **146**, 181–193 (2019).
 25. Kai, M. F. & Dai, J. G. Understanding geopolymer binder-aggregate interfacial characteristics at molecular level. *Cem. Concr. Res.* **149**, 106582 (2021).
 26. Kai, M. F., Ji, W. M. & Dai, J. G. Atomistic insights into the debonding of Epoxy–Concrete interface with water presence. *Eng. Fract. Mech.* **271**, 108668 (2022).
 27. Wang, X. Q., Chow, C. L. & Lau, D. Topology-controlled thermomechanical properties of diamond nanothread enhanced polymeric materials. *Appl. Mater. Today* **32**, 101822 (2023).
 28. Kai, M. F., Xiao, Y., Shuai, X. L. & Ye, G. Compressive Behavior of Engineered Cementitious Composites under High Strain-Rate Loading. *J. Mater. Civil Eng.* **29**, 04016254 (2016).
 29. Wei, H., Liu, T., Zhou, A., Zou, D. & Li, Y. Toughening static and dynamic damping characteristics of ultra-high performance concrete via interfacial modulation approaches. *Cem. Concr. Compos.* **136**, 104879 (2023).
 30. Kai, M. F., Zhang, L. W. & Liew, K. M. New insights into creep characteristics of calcium silicate hydrates at molecular level. *Cem. Concr. Res.* **142**, 106366 (2021).
 31. Kai, M. F., Hou, D. S., Sanchez, F., Poon, C. S. & Dai, J. G. Nanoscale Insights into the Influence of Seawater (NaCl) on the Behavior of Calcium Silicate Hydrate. *J. Phys. Chem. C* **127**, 8735–8750 (2023).
 32. Kai, M. F., Sanchez, F., Hou, D. S. & Dai, J. G. Nanoscale insights into the interfacial characteristics between calcium silicate hydrate and silica. *Appl. Surf. Sci.* **616**, 156478 (2023).
 33. Jian, W. & Lau, D. Understanding the effect of functionalization in CNT-epoxy nanocomposite from molecular level. *Compos. Sci. Technol.* **191**, 108076 (2020).
 34. Jian, W. & Lau, D. Creep performance of CNT-based nanocomposites: A parametric study. *Carbon N. Y.* **153**, 745–756 (2019).
 35. Zhao, D., Wang, X. Q., Tam, L., Chow, C. L. & Lau, D. Tailored twisted CNT bundle with improved inter-tube slipping performances. *Thin Walled Struct.* 111536, <https://doi.org/10.1016/J.TWS.2023.111536> (2023).
 36. Miller, R. E., Tadmor, E. B., Miller, R. E. & Tadmor, E. B. The Quasicontinuum Method: Overview, applications and current directions. *JCMD* **9**, 203–239 (2002).
 37. Zhang, S. et al. Mechanics of defects in carbon nanotubes: Atomistic and multiscale simulations. *Phys. Rev. B Condens. Matter. Mater. Phys.* **71**, 115403 (2005).
 38. Yip, S. & Short, M. P. Multiscale materials modelling at the mesoscale. *Nat. Mater.* **12**, 774–777 (2013).
 39. Liu, T. et al. Atomic insight into the functionalization of cellulose nanofiber on durability of epoxy nanocomposites. *Nano Res.* **16**, 3256–3266 (2023).
 40. Rossi, P. Influence of fibre geometry and matrix maturity on the mechanical performance of ultra high-performance cement-based composites. *Cem. Concr. Compos.* **37**, 246–248 (2013).
 41. Bajaber, M. A. & Hakeem, I. Y. UHPC evolution, development, and utilization in construction: a review. *J. Mater. Res. Technol.* **10**, 1058–1074 (2021).
 42. Huang, L. J., Geng, L. & Peng, H. X. Microstructurally inhomogeneous composites: Is a homogeneous reinforcement distribution optimal? *Prog. Mater. Sci.* **71**, 93–168 (2015).
 43. Mahjoubi, S., Meng, W. & Bao, Y. Auto-tune learning framework for prediction of flowability, mechanical properties, and porosity of ultra-high-performance concrete (UHPC). *Appl. Soft. Comput.* **115**, 108182 (2022).
 44. Meng, W. & Khayat, K. H. Improving flexural performance of ultra-high-performance concrete by rheology control of suspending mortar. *Compos. B Eng.* **117**, 26–34 (2017).
 45. Azreen, N. M., Rashid, R. S. M., Haniza, M., Voo, Y. L. & Mugahed Amran, Y. H. Radiation shielding of ultra-high-performance concrete with silica sand, amang and lead glass. *Constr. Build Mater.* **172**, 370–377 (2018).
 46. Mishra, O. & Singh, S. P. An overview of microstructural and material properties of ultra-high-performance concrete. *J. Sustain. Cem. Based Mater.* **8**, 97–143 (2019).
 47. Wei, H., Zhou, A., Liu, T., Zou, D. & Jian, H. Dynamic and environmental performance of eco-friendly ultra-high performance concrete containing waste cathode ray tube glass as a substitution of river sand. *Resour. Conserv. Recycl.* **162**, 105021 (2020).
 48. Liu, T., Wei, H., Zou, D., Zhou, A. & Jian, H. Utilization of waste cathode ray tube funnel glass for ultra-high performance concrete. *J. Clean. Prod.* **249**, 119333 (2020).
 49. Oh, T. et al. Effect of high-volume substituted nanosilica on the hydration and mechanical properties of Ultra-High-Performance Concrete (UHPC). *Cem. Concr. Res.* **175**, 107379 (2024).
 50. Shafieifar, M., Farzad, M. & Azizinamini, A. Experimental and numerical study on mechanical properties of Ultra High Performance Concrete (UHPC). *Constr. Build Mater.* **156**, 402–411 (2017).
 51. Dils, J., Boel, V. & De Schutter, G. Vacuum mixing technology to improve the mechanical properties of ultra-high performance concrete. *Mater. Struct. Materiaux Constr.* **48**, 3485–3501 (2015).
 52. Sharma, R., Jang, J. G. & Bansal, P. P. A comprehensive review on effects of mineral admixtures and fibers on engineering properties of ultra-high-performance concrete. *J. Build. Eng.* **45**, 103314 (2022).
 53. Yoo, D.-Y., Banthia, N. & Yoon, Y.-S. Recent development of innovative steel fibers for ultra-high-performance concrete (UHPC): A critical review. *Cem. Concr. Compos.* **145**, 105359 (2024).
 54. Karim, R. & Shafei, B. Investigation of Five Synthetic Fibers as Potential Replacements of Steel Fibers in Ultrahigh-Performance Concrete. *J. Mater. Civil Eng.* **34**, 04022126 (2022).
 55. Hannawi, K., Bian, H., Prince-Agbojidan, W. & Raghavan, B. Effect of different types of fibers on the microstructure and the mechanical behavior of Ultra-High Performance Fiber-Reinforced Concretes. *Compos. B Eng.* **86**, 214–220 (2016).
 56. Li, Y., Tan, K. H. & Yang, E. H. Influence of aggregate size and inclusion of polypropylene and steel fibers on the hot permeability of ultra-high performance concrete (UHPC) at elevated temperature. *Constr. Build Mater.* **169**, 629–637 (2018).
 57. Meng, W. & Khayat, K. H. Effect of graphite nanoplatelets and carbon nanofibers on rheology, hydration, shrinkage, mechanical properties, and microstructure of UHPC. *Cem. Concr. Res.* **105**, 64–71 (2018).
 58. Meng, W. & Khayat, K. H. Mechanical properties of ultra-high-performance concrete enhanced with graphite nanoplatelets and carbon nanofibers. *Compos. B Eng.* **107**, 113–122 (2016).
 59. Wang, W., Chen, S. J., Sagoe-Crentsil, K. & Duan, W. Graphene oxide-reinforced thin shells for high-performance, lightweight cement composites. *Compos. B Eng.* **235**, 109796 (2022).
 60. Fang, Z. et al. Research on mechanical properties and hydration characteristics of ultra-high performance concrete with high-volume fly ash microsphere. *J. Build. Eng.* **78**, 107738 (2023).
 61. Zelić, J., Rušić, D., Veža, D. & Krstulović, R. The role of silica fume in the kinetics and mechanisms during the early stage of cement hydration. *Cem. Concr. Res.* **30**, 1655–1662 (2000).
 62. Van Tuan, N., Ye, G., Van Breugel, K. & Copuroglu, O. Hydration and microstructure of ultra high performance concrete incorporating rice husk ash. *Cem. Concr. Res.* **41**, 1104–1111 (2011).
 63. Lau, D. & Büyükoztürk, O. Fracture characterization of concrete/epoxy interface affected by moisture. *Mech. Mater.* **42**, 1031–1042 (2010).

64. Zhuang, W., Li, S., Deng, Q., Chen, M. & Yu, Q. Effects of coarse aggregates size on dynamic characteristics of ultra-high performance concrete: Towards enhanced impact resistance. *Constr. Build Mater.* **411**, 134524 (2024).
65. Luo, Z. et al. Effects of different nanomaterials on the early performance of ultra-high performance concrete (UHPC): C–S–H seeds and nano-silica. *Cem. Concr. Compos.* **142**, 105211 (2023).
66. Wu, R. et al. Degradation of fiber/matrix interface under various environmental and loading conditions: Insights from molecular simulations. *Constr. Build Mater.* **390**, 131101 (2023).
67. Wang, X. Q., Jian, W., Buyukozturk, O., Leung, C. K. Y. & Lau, D. Degradation of epoxy/glass interface in hygrothermal environment: An atomistic investigation. *Compos. B Eng.* **206**, 108534 (2021).
68. Wang, X. Q., Büyüköztürk, O., Leung, C. K. Y. & Lau, D. Atomistic prediction on the degradation of vinyl ester-based composite under chloride and elevated temperature. *Compos. Sci. Technol.* **226**, 109539 (2022).
69. Qi, J., Cheng, Z., John Ma, Z., Wang, J. & Liu, J. Bond strength of reinforcing bars in ultra-high performance concrete: Experimental study and fiber–matrix discrete model. *Eng. Struct.* **248**, 113290 (2021).
70. Yoo, D. Y., Park, J. J. & Kim, S. W. Fiber pullout behavior of HPFRCC: Effects of matrix strength and fiber type. *Compos. Struct.* **174**, 263–276 (2017).
71. Zhou, A., Qiu, Q., Chow, C. L. & Lau, D. Interfacial performance of aramid, basalt and carbon fiber reinforced polymer bonded concrete exposed to high temperature. *Compos. Part A Appl. Sci. Manuf.* **131**, 105802 (2020).
72. Robins, P., Austin, S. & Jones, P. Pull-out behaviour of hooked steel fibres. *Mater. Struct. Matériaux et Constr.* **35**, 434–442 (2002).
73. Li, Y. et al. Modelling method of fibre distribution in steel fibre reinforced concrete based on X-ray image recognition. *Compos. B Eng.* **223**, 109124 (2021).
74. Feng, J., Sun, W. W., Wang, X. M. & Shi, X. Y. Mechanical analyses of hooked fiber pullout performance in ultra-high-performance concrete. *Constr. Build Mater.* **69**, 403–410 (2014).
75. Qi, J., Wu, Z., Ma, Z. J. & Wang, J. Pullout behavior of straight and hooked-end steel fibers in UHPC matrix with various embedded angles. *Constr. Build Mater.* **191**, 764–774 (2018).
76. Zhang, H., Ji, T. & Lin, X. Pullout behavior of steel fibers with different shapes from ultra-high performance concrete (UHPC) prepared with granite powder under different curing conditions. *Constr. Build Mater.* **211**, 688–702 (2019).
77. Yoo, D. Y. & Kim, S. Comparative pullout behavior of half-hooked and commercial steel fibers embedded in UHPC under static and impact loads. *Cem. Concr. Compos.* **97**, 89–106 (2019).
78. Cao, Y. Y. & Yu, Q. L. Effect of inclination angle on hooked end steel fiber pullout behavior in ultra-high performance concrete. *Compos. Struct.* **201**, 151–160 (2018).
79. Deng, Y., Zhang, Z., Shi, C., Wu, Z. & Zhang, C. Steel Fiber–Matrix Interfacial Bond in Ultra-High Performance Concrete: A Review. *Engineering* **22**, 215–232 (2023).
80. Yoo, D. Y., Chun, B. & Kim, J. J. Bond performance of abraded arch-type steel fibers in ultra-high-performance concrete. *Cem. Concr. Compos.* **109**, 103538 (2020).
81. Shen, P., Lu, L., He, Y., Wang, F. & Hu, S. The effect of curing regimes on the mechanical properties, nano-mechanical properties and microstructure of ultra-high performance concrete. *Cem. Concr. Res.* **118**, 1–13 (2019).
82. Kahanji, C., Ali, F., Nadjai, A. & Alam, N. Effect of curing temperature on the behaviour of UHPFRC at elevated temperatures. *Constr. Build Mater.* **182**, 670–681 (2018).
83. Shannag, M. J., Brincker, R. & Hansen, W. Pullout behavior of steel fibers from cement-based composites. *Cem. Concr. Res.* **27**, 925–936 (1997).
84. Huang, H., Gao, X., Li, L. & Wang, H. Improvement effect of steel fiber orientation control on mechanical performance of UHPC. *Constr. Build Mater.* **188**, 709–721 (2018).
85. Huang, H., Gao, X. & Teng, L. Fiber alignment and its effect on mechanical properties of UHPC: An overview. *Constr. Build Mater.* **296**, 123741 (2021).
86. Yu, J., Zhang, B., Chen, W. & Liu, H. Multi-scale analysis on the tensile properties of UHPC considering fiber orientation. *Compos. Struct.* **280**, 114835 (2022).
87. Teng, L., Huang, H., Khayat, K. H. & Gao, X. Simplified analytical model to assess key factors influenced by fiber alignment and their effect on tensile performance of UHPC. *Cem. Concr. Compos.* **127**, 104395 (2022).
88. Zhou, B. & Uchida, Y. Influence of flowability, casting time and formwork geometry on fiber orientation and mechanical properties of UHPFRC. *Cem. Concr. Res.* **95**, 164–177 (2017).
89. Kang, S. T. & Kim, J. K. The relation between fiber orientation and tensile behavior in an Ultra High Performance Fiber Reinforced Cementitious Composites (UHPFRCC). *Cem. Concr. Res.* **41**, 1001–1014 (2011).
90. Yoo, D. Y., Shin, W., Chun, B. & Banthia, N. Assessment of steel fiber corrosion in self-healed ultra-high-performance fiber-reinforced concrete and its effect on tensile performance. *Cem. Concr. Res.* **133**, 106091 (2020).
91. Wang, P., Ke, L., Wen, Y., Wu, H., Hao-liang, W. & Leung, C. K. Y. Lowering exposure pH for durability enhancement of glass fiber reinforcement polymer (GFRP) rebars. *Constr. Build Mater.* **354**, 129131 (2022).
92. Wang, P. et al. Mechanical properties and microstructure of glass fiber reinforced polymer (GFRP) rebars embedded in carbonated reactive MgO-based concrete (RMC). *Cem. Concr. Compos.* **142**, 105207 (2023).
93. Qin, R. & Denvid, L. Evaluation of the Moisture Effect on the Material Interface Using Multiscale Modeling. *Multisc. Sci. Eng.* **1**, 108–118 (2019).
94. Qureshi, T. S. & Panesar, D. K. Nano reinforced cement paste composite with functionalized graphene and pristine graphene nanoplatelets. *Compos. B Eng.* **197**, 108063 (2020).
95. Zhang, J., Chevali, V. S., Wang, H. & Wang, C. H. Current status of carbon fibre and carbon fibre composites recycling. *Compos. B Eng.* **193**, 108053 (2020).
96. Reda, M. M., Shrive, N. G. & Gillott, J. E. Microstructural investigation of innovative UHPC. *Cem. Concr. Res.* **29**, 323–329 (1999).
97. Qin, R., Zhou, A., Yu, Z., Wang, Q. & Lau, D. Role of carbon nanotube in reinforcing cementitious materials: An experimental and coarse-grained molecular dynamics study. *Cem. Concr. Res.* **147**, 106517 (2021).
98. Liu, J., Farzadnia, N. & Shi, C. Effects of superabsorbent polymer on interfacial transition zone and mechanical properties of ultra-high performance concrete. *Constr. Build Mater.* **231**, 117142 (2020).
99. Huang, H. et al. Micromechanical properties of interfacial transition zone between carbon fibers and UHPC matrix based on nano-scratching tests. *Cem. Concr. Compos.* **139**, 105014 (2023).
100. Yu, K. Q. et al. Micro-structural and mechanical properties of ultra-high performance engineered cementitious composites (UHP-ECC) incorporation of recycled fine powder (RFP). *Cem. Concr. Res.* **124**, 105813 (2019).
101. Oh, T., You, I., Banthia, N. & Yoo, D. Y. Deposition of nanosilica particles on fiber surface for improving interfacial bond and tensile performances of ultra-high-performance fiber-reinforced concrete. *Compos. B Eng.* **221**, 109030 (2021).
102. Li, Y., Tan, K. H. & Yang, E. H. Synergistic effects of hybrid polypropylene and steel fibers on explosive spalling prevention of ultra-high performance concrete at elevated temperature. *Cem. Concr. Compos.* **96**, 174–181 (2019).

103. Li, Y., Zhang, Y., Yang, E. H. & Tan, K. H. Effects of geometry and fraction of polypropylene fibers on permeability of ultra-high performance concrete after heat exposure. *Cem. Concr. Res.* **116**, 168–178 (2019).
104. Khandelwal, S. & Rhee, K. Y. Recent advances in basalt-fiber-reinforced composites: Tailoring the fiber-matrix interface. *Compos. B Eng.* **192**, 108011 (2020).
105. Chen, Z. et al. Spalling resistance and mechanical properties of ultra-high performance concrete reinforced with multi-scale basalt fibers and hybrid fibers under elevated temperature. *J. Build. Eng.* **77**, 107435 (2023).
106. He, Z. et al. Effect of wollastonite microfibers as cement replacement on the properties of cementitious composites: A review. *Constr. Build Mater.* **261**, 119920 (2020).
107. Ajoku, C. A., Turatsinze, A. & Abou-Chakra, A. Mechanical behaviour of wollastonite-based cement composites incorporating fibres and recycled rubber aggregates. *Constr. Build Mater.* **392**, 131843 (2023).
108. Khan, M., Lao, J., Ahmad, M. R. & Dai, J. G. Influence of high temperatures on the mechanical and microstructural properties of hybrid steel-basalt fibers based ultra-high-performance concrete (UHPC). *Constr. Build Mater.* **411**, 134387 (2024).
109. Hao, H., Chow, C. L. & Lau, D. Carbon monoxide release mechanism in cellulose combustion using reactive forcefield. *Fuel* **269**, 117422 (2020).
110. Hao, H., Chow, C. L. & Lau, D. Effect of heat flux on combustion of different wood species. *Fuel* **278**, 118325 (2020).
111. Wu, L., Farzadnia, N., Shi, C., Zhang, Z. & Wang, H. Autogenous shrinkage of high performance concrete: A review. *Constr. Build Mater.* **149**, 62–75 (2017).
112. Xu, H. et al. Experimental study on durability of fiber reinforced concrete: Effect of cellulose fiber, polyvinyl alcohol fiber and polyolefin fiber. *Constr. Build Mater.* **306**, 124867 (2021).
113. Niu, Y., Wei, J. & Jiao, C. Crack propagation behavior of ultra-high-performance concrete (UHPC) reinforced with hybrid steel fibers under flexural loading. *Constr. Build Mater.* **294**, 123510 (2021).
114. Wu, Z., Shi, C., He, W. & Wang, D. Static and dynamic compressive properties of ultra-high performance concrete (UHPC) with hybrid steel fiber reinforcements. *Cem. Concr. Compos.* **79**, 148–157 (2017).
115. Sun, W., Chen, H., Luo, X. & Qian, H. The effect of hybrid fibers and expansive agent on the shrinkage and permeability of high-performance concrete. *Cem. Concr. Res.* **31**, 595–601 (2001).
116. Xie, C., Cao, M., Guan, J., Liu, Z. & Khan, M. Improvement of boundary effect model in multi-scale hybrid fibers reinforced cementitious composite and prediction of its structural failure behavior. *Compos. B Eng.* **224**, 109219 (2021).
117. Meng, W. & Khayat, K. H. Effect of Hybrid Fibers on Fresh Properties, Mechanical Properties, and Autogenous Shrinkage of Cost-Effective UHPC. *J. Mater. Civil Eng.* **30**, 04018030 (2018).
118. Huang, L., Xu, L., Chi, Y. & Xu, H. Experimental investigation on the seismic performance of steel–polypropylene hybrid fiber reinforced concrete columns. *Constr. Build Mater.* **87**, 16–27 (2015).
119. Chen, X. et al. Experimental studies and microstructure analysis for ultra high-performance reactive powder concrete. *Constr. Build Mater.* **229**, 116924 (2019).
120. Yoo, D. Y., Oh, T. & Banthia, N. Nanomaterials in ultra-high-performance concrete (UHPC) – A review. *Cem. Concr. Compos.* **134**, 104730 (2022).
121. Farajzadehha, S., Ziaei Moayed, R. & Mahdikhani, M. Comparative study on uniaxial and triaxial strength of plastic concrete containing nano silica. *Constr. Build Mater.* **244**, 118212 (2020).
122. Alhawati, M. & Ashour, A. Bond strength between corroded steel and recycled aggregate concrete incorporating nano silica. *Constr. Build Mater.* **237**, 117441 (2020).
123. Wang, P. et al. Mechanical and long-term durability prediction of GFRP rebars with the adoption of low-pH CSA concrete. *Constr. Build Mater.* **346**, 128444 (2022).
124. Wang, P., Ke, L. Y. W., Hao-liang, W. & Leung, C. K. Y. Effects of water-to-cement ratio on the performance of concrete and embedded GFRP reinforcement. *Constr. Build Mater.* **351**, 128833 (2022).
125. Saeki, T. & Monteiro, P. J. M. A model to predict the amount of calcium hydroxide in concrete containing mineral admixtures. *Cem. Concr. Res.* **35**, 1914–1921 (2005).
126. Yu, J., Zhang, B., Chen, W. & He, J. Experimental and multi-scale numerical investigation of ultra-high performance fiber reinforced concrete (UHPC) with different coarse aggregate content and fiber volume fraction. *Constr. Build Mater.* **260**, 120444 (2020).
127. Shao, R., Wu, C., Li, J. & Liu, Z. Investigation on the mechanical characteristics of multiscale mono/hybrid steel fibre-reinforced dry UHPC. *Cem. Concr. Compos.* **133**, 104681 (2022).
128. Zhang, Y., Ju, J. W., Zhu, H. & Yan, Z. A novel multi-scale model for predicting the thermal damage of hybrid fiber-reinforced concrete. *Int. J. Damage Mech.* **29**, 19–44 (2020).
129. Feng, J. et al. Influence of fiber mixture on impact response of ultra-high-performance hybrid fiber reinforced cementitious composite. *Compos. B Eng.* **163**, 487–496 (2019).
130. Zhao, S., Liu, R., Liu, J. & Yang, L. Comparative study on the effect of steel and plastic synthetic fibers on the dynamic compression properties and microstructure of ultra-high-performance concrete (UHPC). *Compos. Struct.* **324**, 117570 (2023).
131. Lau, D., Büyüköztürk, O. & Buehler, M. J. Multiscale modeling of organic-inorganic interface: From molecular dynamics simulation to finite element modeling. *MRS Online Proc. Library* **1466**, 44–49 (2012).
132. Lau, D., Büyüköztürk, O. & Buehler, M. J. Characterization of the intrinsic strength between epoxy and silica using a multiscale approach. *J. Mater. Res.* **27**, 1787–1796 (2012).
133. Lau, D., Broderick, K., Buehler, M. J. & Büyüköztürk, O. A robust nanoscale experimental quantification of fracture energy in a bilayer material system. *Proc. Natl Acad. Sci. USA* **111**, 11990–11995 (2014).
134. Shilkrot, L. E., Miller, R. E. & Curtin, W. A. Multiscale plasticity modeling: coupled atomistics and discrete dislocation mechanics. *J. Mech. Phys. Solids* **52**, 755–787 (2004).
135. Karapiperis, K., Stainier, L., Ortiz, M. & Andrade, J. E. Data-Driven multiscale modeling in mechanics. *J. Mech. Phys. Solids* **147**, 104239 (2021).
136. Filla, N., Hou, J., Li, H. & Wang, X. A multiscale framework for modeling fibrin fiber networks: Theory development and validation. *J. Mech. Phys. Solids* **179**, 105392 (2023).
137. Ahmad, R., Liu, M., Ortiz, M., Mukerji, T. & Cai, W. Computation of effective elastic moduli of rocks using hierarchical homogenization. *J. Mech. Phys. Solids* **174**, 105268 (2023).
138. Michopoulos, J. G., Farhat, C. & Fish, J. Modeling and Simulation of Multiphysics Systems. *J. Comput. Inf. Sci. Eng.* **5**, 198–213 (2005).
139. Brini, E. & Van Der Vegt, N. F. A. Chemically transferable coarse-grained potentials from conditional reversible work calculations. *J. Chem. Phys.* **137**, 154113 (2012).
140. Mullinax, J. W. & Noid, W. G. Extended ensemble approach for deriving transferable coarse-grained potentials. *J. Chem. Phys.* **131**, 104110 (2009).
141. De Jong, D. H. et al. Improved parameters for the martini coarse-grained protein force field. *J. Chem. Theory Comput.* **9**, 687–697 (2013).
142. Yu, Z. & Lau, D. Nano- and mesoscale modeling of cement matrix. *Nanoscale Res. Lett.* **10**, 1–6 (2015).
143. Yu, Z., Zhou, A. & Lau, D. Mesoscopic packing of disk-like building blocks in calcium silicate hydrate. *Sci. Rep.* **6**, 1–8 (2016).

144. Ladevèze, P., Passieux, J. C. & Néron, D. The LATIN multiscale computational method and the Proper Generalized Decomposition. *Comput. Methods Appl. Mech. Eng.* **199**, 1287–1296 (2010).
145. Budarapu, P. R., Zhuang, X., Rabczuk, T. & Bordas, S. P. A. Multiscale modeling of material failure: Theory and computational methods. *Adv. Appl. Mech.* **52**, 1–103 (2019).
146. Wang, J. Cohesive zone model of FRP-concrete interface debonding under mixed-mode loading. *Int. J. Solids Struct.* **44**, 6551–6568 (2007).
147. Park, K., Ha, K., Choi, H. & Lee, C. Prediction of interfacial fracture between concrete and fiber reinforced polymer (FRP) by using cohesive zone modeling. *Cem. Concr. Compos.* **63**, 122–131 (2015).
148. Wu, T. & Wriggers, P. Multiscale diffusion-thermal-mechanical cohesive zone model for concrete. *Comput. Mech.* **55**, 999–1016 (2015).
149. Nairn, J. A. & Aimene, Y. E. A re-evaluation of mixed-mode cohesive zone modeling based on strength concepts instead of traction laws. *Eng. Fract. Mech.* **248**, 107704 (2021).
150. Shi, T., Zhang, Y., Zhang, X., Wang, Y. & Zheng, K. A strength based thermo-mechanical coupled cohesive zone model for simulating heat flux induced interface debonding. *Compos. Sci. Technol.* **243**, 110255 (2023).
151. Qu, S. et al. Prediction of tensile response of UHPC with aligned and ZnPh treated steel fibers based on a spatial stochastic process. *Cem. Concr. Res.* **136**, 106165 (2020).
152. Al-Ameen, E., Blanco, A. & Cavalaro, S. Durability, permeability, and mechanical performance of sprayed UHPC, as an attribute of fibre content and geometric stability. *Constr. Build Mater.* **407**, 133393 (2023).
153. Haile, B. F., Jin, D. W., Yang, B., Park, S. & Lee, H. K. Multi-level homogenization for the prediction of the mechanical properties of ultra-high-performance concrete. *Constr. Build Mater.* **229**, 116797 (2019).
154. Hollingsworth, S. A. & Dror, R. O. Review Molecular Dynamics Simulation for All. *Neuron* **99**, 1129–1143 (2018).
155. Karplus, M. & Petsko, G. A. Molecular dynamics simulations in biology. *Nature* **347**, 631–639 (1990).
156. Togo, A. & Tanaka, I. First principles phonon calculations in materials science. *Scr. Mater.* **108**, 1–5 (2015).
157. Wang, X. Q. & Lau, D. Atomistic investigation of GFRP composites under chloride environment. *Adv. Struct. Eng.* **24**, 1138–1149 (2021).
158. Eftekhari, M., Hatefi Ardakani, S. & Mohammadi, S. An XFEM multiscale approach for fracture analysis of carbon nanotube reinforced concrete. *Theor. Appl. Fract. Mech.* **72**, 64–75 (2014).
159. Wu, L., Liu, P., Zhang, Z., Zhu, D. & Wang, H. Multiscale modeling for high-performance concrete: A review. *Int. J. Multisc. Comput. Eng.* **16**, 267–283 (2018).
160. Nie, F., Cheuk, , Chow, L. & Lau, D. A Review on Multiscale Modeling of Asphalt: Development and Applications. *Multisc. Sci. Eng.* **4**, 10–27 (2022).
161. Nie, F., Jian, W., Yu, Z., Chow, C. L. & Lau, D. Mesoscale modeling to study isolated asphaltene agglomerates. *Constr. Build Mater.* **379**, 131249 (2023).
162. Gracie, R. & Belytschko, T. Concurrently coupled atomistic and XFEM models for dislocations and cracks. *Int. J. Numer Methods Eng.* **78**, 354–378 (2009).
163. Miller, R. E. & Tadmor, E. B. A unified framework and performance benchmark of fourteen multiscale atomistic/continuum coupling methods. *Model. Simul. Mat. Sci. Eng.* **17**, 053001 (2009).
164. Kohlhoff, S., Gumbsch, P. & Fischmeister, H. F. Crack propagation in b.c.c. crystals studied with a combined finite-element and atomistic model. *Philosoph. Mag. A* **64**, 851–878 (1991).
165. Shilkrot, L. E., Curtin, W. A. & Miller, R. E. A coupled atomistic/continuum model of defects in solids. *J. Mech. Phys. Solids* **50**, 2085–2106 (2002).
166. Shilkrot, L. E., Miller, R. E. & Curtin, W. A. Coupled Atomistic and Discrete Dislocation Plasticity. *Phys. Rev. Lett.* **89**, 025501 (2002).
167. Abraham, F. F., Broughton, J. Q., Bernstein, N. & Kaxiras, E. Spanning the length scales in dynamic simulation. *Comput. Phys.* **12**, 538–546 (1998).
168. Broughton, J. Q., Abraham, F. F., Bernstein, N. & Kaxiras, E. Concurrent coupling of length scales: Methodology and application. *Phys. Rev. B* **60**, 2391 (1999).
169. Liu, B., Huang, Y., Jiang, H., Qu, S. & Hwang, K. C. The atomic-scale finite element method. *Comput. Methods Appl. Mech. Eng.* **193**, 1849–1864 (2004).
170. Liu, B. et al. Atomic-scale finite element method in multiscale computation with applications to carbon nanotubes. *Phys. Rev. B Condens. Matter. Mater. Phys.* **72**, 035435 (2005).
171. Wang, P., Ke, L. Y. W., Hao-liang, W. & Leung, C. K. Y. Hygrothermal aging effect on the water diffusion in glass fiber reinforced polymer (GFRP) composite: Experimental study and numerical simulation. *Compos. Sci. Technol.* **230**, 109762 (2022).
172. Honglai, T. & Wei, Y. Atomistic/continuum simulation of interfacial fracture part I: Atomistic simulation. *Acta Mech. Sin.* **10**, 150–161 (1994).
173. Kadowaki, H. & Liu, W. K. Bridging multi-scale method for localization problems. *Comput. Methods Appl. Mech. Eng.* **193**, 3267–3302 (2004).
174. Xiao, S. P. & Belytschko, T. A bridging domain method for coupling continua with molecular dynamics. *Comput. Methods Appl. Mech. Eng.* **193**, 1645–1669 (2004).
175. Pawar, S., Ahmed, S. E. & San, O. Interface learning in fluid dynamics: Statistical inference of closures within micro-macro-coupling models. *Phys. Fluids* **32**, 091704 (2020).
176. Rodrigues, E. A., Manzoli, O. L. & Bitencourt, L. A. G. 3D concurrent multiscale model for crack propagation in concrete. *Comput. Methods Appl. Mech. Eng.* **361**, 112813 (2020).
177. Elliott, J. A. Novel approaches to multiscale modelling in materials science. *Int. Mater. Rev.* **56**, 207–225 (2011).
178. Knap, J. & Ortiz, M. An analysis of the quasicontinuum method. *J. Mech. Phys. Solids* **49**, 1899–1923 (2001).
179. Yaphary, Y. L., Sanchez, F., Lau, D. & Poon, C. S. Mechanical properties of colloidal calcium-silicate-hydrate gel with different gel-pore ionic solutions: A mesoscale study. *Microporous Mesoporous Mater.* **316**, 110944 (2021).
180. Wang, H., Hu, M., Xia, M., Ke, F. & Bai, Y. Molecular/cluster statistical thermodynamics methods to simulate quasi-static deformations at finite temperature. *Int. J. Solids Struct.* **45**, 3918–3933 (2008).
181. Ioannidou, K. et al. Mesoscale texture of cement hydrates. *Proc. Natl Acad. Sci. USA* **113**, 2029–2034 (2016).
182. Sindu, B. S. & Sasmal, S. Molecular dynamics simulations for evaluation of surfactant compatibility and mechanical characteristics of carbon nanotubes incorporated cementitious composite. *Constr. Build Mater.* **253**, 119190 (2020).
183. Eftekhari, M. & Mohammadi, S. Molecular dynamics simulation of the nonlinear behavior of the CNT-reinforced calcium silicate hydrate (C–S–H) composite. *Compos. Part A Appl. Sci. Manuf.* **82**, 78–87 (2016).
184. Yu, Z. et al. Coarse-grained molecular dynamics study on submicron structuring of calcium silicate hydrate with enhanced tensile modulus and strength. *J. Build. Eng.* **82**, 108271 (2024).
185. Rudd, R. E. & Broughton, J. Q. Coarse-grained molecular dynamics: Nonlinear finite elements and finite temperature. *Phys. Rev. B Condens. Matter. Mater. Phys.* **72**, 144104 (2005).
186. Worrell, E., Price, L., Martin, N., Hendriks, C. & Meida, L. O. Carbon dioxide emissions from the global cement industry. *Ann. Rev. Energy Environ.* **26**, 303–329 (2003).
187. Mosaberpanah, M. A. & Eren, O. CO₂-full factorial optimization of an ultra-high performance concrete mix design. *Eur. J. Environ. Civil Eng.* **22**, 450–463 (2018).

188. Kromoser, B., Preinstorfer, P. & Kollegger, J. Building lightweight structures with carbon-fiber-reinforced polymer-reinforced ultra-high-performance concrete: Research approach, construction materials, and conceptual design of three building components. *Struct. Concrete* **20**, 730–744 (2019).
189. Teng, L., Addai-Nimoh, A. & Khayat, K. H. Effect of lightweight sand and shrinkage reducing admixture on structural build-up and mechanical performance of UHPC. *J. Build. Eng.* **68**, 106144 (2023).
190. Isa, M. N., Pilakoutas, K., Guadagnini, M. & Angelakopoulos, H. Mechanical performance of affordable and eco-efficient ultra-high performance concrete (UHPC) containing recycled tyre steel fibres. *Constr. Build Mater.* **255**, 119272 (2020).
191. Qian, D. et al. A novel development of green ultra-high performance concrete (UHPC) based on appropriate application of recycled cementitious material. *J. Clean. Prod.* **261**, 121231 (2020).
192. Yu, R., Spiesz, P. & Brouwers, H. J. H. Development of an eco-friendly Ultra-High Performance Concrete (UHPC) with efficient cement and mineral admixtures uses. *Cem. Concr. Compos.* **55**, 383–394 (2015).
193. Zhou, A. et al. A novel approach for recycling engineering sediment waste as sustainable supplementary cementitious materials. *Resour. Conserv. Recycl.* **167**, 105435 (2021).
194. Zhou, A. et al. Recycling and optimum utilization of engineering sediment waste into low-carbon geopolymer paste for sustainable infrastructure. *J. Clean Prod.* **383**, 135549 (2023).
195. Tafrroui, A., Escadeillas, G., Lebailli, S. & Vidal, T. Metakaolin in the formulation of UHPC. *Constr. Build. Mater.* **23**, 669–674 (2009).
196. Wu, Z., Khayat, K. H. & Shi, C. Changes in rheology and mechanical properties of ultra-high performance concrete with silica fume content. *Cem. Concr. Res.* **123**, 105786 (2019).
197. Liu, T., Wei, H., Zhou, A., Zou, D. & Jian, H. Multiscale investigation on tensile properties of ultra-high performance concrete with silane coupling agent modified steel fibers. *Cem. Concr. Compos.* **111**, 103638 (2020).
198. Chen, H., Qin, R., Chow, C. L. & Lau, D. Recycling thermoset plastic waste for manufacturing green cement mortar. *Cem. Concr. Compos.* **137**, 104922 (2023).
199. Essam, A., Mostafa, S. A., Khan, M. & Tahwia, A. M. Modified particle packing approach for optimizing waste marble powder as a cement substitute in high-performance concrete. *Constr. Build Mater.* **409**, 133845 (2023).
200. Chen, H., Chow, C. L. & Lau, D. Developing green and sustainable concrete in integrating with different urban wastes. *J. Clean. Prod.* **368**, 133057 (2022).
201. Liu, J., Hu, N., Chow, C. L. & Lau, D. Unfolding behavior of self-folded boron nitride nanosheets inducing ductility of cementitious composites. *Appl. Surf. Sci.* **599**, 153818 (2022).
202. Lee, J. Y., Yuan, T., Shin, H. O. & Yoon, Y. S. Strategic use of steel fibers and stirrups on enhancing impact resistance of ultra-high-performance fiber-reinforced concrete beams. *Cem. Concr. Compos.* **107**, 103499 (2020).
203. Rahmati, M. & Toufigh, V. Evaluation of geopolymer concrete at high temperatures: An experimental study using machine learning. *J. Clean. Prod.* **372**, 133608 (2022).
204. Bouhaya, L., Le Roy, R. & Feraille-Fresnet, A. Simplified environmental study on innovative bridge structure. *Environ. Sci. Technol.* **43**, 2066–2071 (2009).
205. Stengel, T. & Schießl, P. Sustainable construction with UHPC—from life cycle inventory data collection to environmental impact assessment. *Proceedings of the 2nd international symposium on ultra high*. Kassel University Press, Kassel. 461–468 (2008).
206. Habert, G. et al. Reducing environmental impact by increasing the strength of concrete: quantification of the improvement to concrete bridges. *J. Clean. Prod.* **35**, 250–262 (2012).
207. Habert, G., Denarié, E., Šajna, A. & Rossi, P. Lowering the global warming impact of bridge rehabilitations by using Ultra High Performance Fibre Reinforced Concretes. *Cem. Concr. Compos.* **38**, 1–11 (2013).
208. Maxwell, D. & Van der Vorst, R. Developing sustainable products and services. *J. Clean. Prod.* **11**, 883–895 (2003).
209. Kaliyavaradhan, S. K. & Ling, T. C. Potential of CO₂ sequestration through construction and demolition (C&D) waste—An overview. *J. CO₂ Utilization* **20**, 234–242 (2017).
210. Karim, R., Najimi, M. & Shafei, B. Assessment of transport properties, volume stability, and frost resistance of non-proprietary ultra-high performance concrete. *Constr. Build Mater.* **227**, 117031 (2019).
211. Ravikumar, D. et al. Carbon dioxide utilization in concrete curing or mixing might not produce a net climate benefit. *Nat. Commun.* **12**, 1–13 (2021).
212. Hung, C.-C., El-Tawil, S. & Chao, S.-H. A Review of Developments and Challenges for UHPC in Structural Engineering: Behavior, Analysis, and Design. *J. Struct. Eng.* **147**, 03121001 (2021).
213. Park, S. H., Kim, D. J., Ryu, G. S. & Koh, K. T. Tensile behavior of Ultra High Performance Hybrid Fiber Reinforced Concrete. *Cem. Concr. Compos.* **34**, 172–184 (2012).
214. Toutlemonde, F. et al. French standards for ultra-high performance fiber-reinforced concrete (UHPRC). *fib Symposium* 1601–1609, https://doi.org/10.1007/978-3-319-59471-2_184 (2018).
215. Wang, X. Q., Chen, P., Chow, C. L. & Lau, D. Artificial-intelligence-led revolution of construction materials: From molecules to Industry 4.0. *Matter* **6**, 1831–1859 (2023).
216. Xu, L., Fan, D., Liu, K., Xu, W. & Yu, R. A machine learning framework for intelligent development of Ultra-High performance concrete (UHPC): From dataset cleaning to performance predicting. *Expert. Syst. Appl.* **242**, 122790 (2024).
217. Nguyen, N. H., Abellán-García, J., Lee, S. & Vo, T. P. From machine learning to semi-empirical formulas for estimating compressive strength of Ultra-High Performance Concrete. *Expert Syst. Appl.* **237**, 121456 (2024).
218. Le, T. T. et al. Mix design and fresh properties for high-performance printing concrete. *Mater. Struct. Materiaux Constr.* **45**, 1221–1232 (2012).
219. Lim, S. et al. Developments in construction-scale additive manufacturing processes. *Autom. Constr.* **21**, 262–268 (2012).
220. Libonati, F., Gu, G. X., Qin, Z., Vergani, L. & Buehler, M. J. Bone-Inspired Materials by Design: Toughness Amplification Observed Using 3D Printing and Testing. *Adv. Eng. Mater.* **18**, 1354–1363 (2016).
221. Smaldone, R. A., Brown, K. A., Gu, G. X. & Ke, C. Using 3D printing as a research tool for materials discovery. *Device* **1**, 100014 (2023).
222. El-Sayegh, S., Romdhane, L. & Manjikian, S. A critical review of 3D printing in construction: benefits, challenges, and risks. *Arch. Civil Mech. Eng.* **20**, 1–25 (2020).
223. Xi, B., Huang, Z., Al-Obaidi, S. & Ferrara, L. Healing capacity of Ultra High Performance Concrete under sustained through crack tensile stresses and aggressive environments. *Cem. Concr. Compos.* **145**, 105355 (2024).
224. Van Tuan, N., Ye, G., Van Breugel, K., Fraaij, A. L. A. & Bui, D. D. The study of using rice husk ash to produce ultra high performance concrete. *Constr. Build Mater.* **25**, 2030–2035 (2011).
225. Zhu, B. et al. Development of 3D printable engineered cementitious composites with ultra-high tensile ductility for digital construction. *Mater. Des.* **181**, 108088 (2019).
226. Fan, D. et al. Intelligent design and manufacturing of ultra-high performance concrete (UHPC) – A review. *Constr. Build Mater.* **385**, 131495 (2023).

Acknowledgements

The work described in this paper was supported by a grant from the Research Grants Council of the Hong Kong Special Administrative Region, China (Project No. CityU R1018-22).

Author contributions

X.Q.W. C.L.C. and D.L. contributed to the conceptualization and manuscript. C.L.C and D. L contributed to the funding acquisition and supervision. All authors reviewed and approved the final manuscript.

Competing interests

The authors declare no competing interests.

Additional information

Correspondence and requests for materials should be addressed to Dervid Lau.

Reprints and permissions information is available at <http://www.nature.com/reprints>

Publisher's note Springer Nature remains neutral with regard to jurisdictional claims in published maps and institutional affiliations.

Open Access This article is licensed under a Creative Commons Attribution 4.0 International License, which permits use, sharing, adaptation, distribution and reproduction in any medium or format, as long as you give appropriate credit to the original author(s) and the source, provide a link to the Creative Commons licence, and indicate if changes were made. The images or other third party material in this article are included in the article's Creative Commons licence, unless indicated otherwise in a credit line to the material. If material is not included in the article's Creative Commons licence and your intended use is not permitted by statutory regulation or exceeds the permitted use, you will need to obtain permission directly from the copyright holder. To view a copy of this licence, visit <http://creativecommons.org/licenses/by/4.0/>.

© The Author(s) 2024